

Targeting an Aromatic Hotspot in *Plasmodium falciparum* 1-Deoxy-D-xylulose-5-phosphate Reductoisomerase with β -Arylpropyl Analogues of Fosmidomycin

Sanjeevani Sooriyaarachchi^{+, [a]}, René Chofor^{+, [b]}, Martijn D. P. Risseeuw,^[b] Terese Bergfors,^[a] Jenny Pouyez,^[c] Cynthia S. Dowd,^[d] Louis Maes,^[e] Johan Wouters,^[c] T. Alwyn Jones,^[a] Serge Van Calenbergh^{+, *[b]} and Sherry L. Mowbray^{+, *[a]}

Blocking the 2-C-methyl-D-erythritol-4-phosphate pathway for isoprenoid biosynthesis offers new ways to inhibit the growth of *Plasmodium* spp. Fosmidomycin [(3-(*N*-hydroxyformamido)propyl)phosphonic acid, **1**] and its acetyl homologue FR-900098 [(3-(*N*-hydroxyacetamido)propyl)phosphonic acid, **2**] potently inhibit 1-deoxy-D-xylulose-5-phosphate reductoisomerase (Dxr), a key enzyme in this biosynthetic pathway. Arylpropyl substituents were introduced at the β -position of the hydroxamate analogue of **2** to study changes in lipophilicity, as well as electronic and steric properties. The potency of several new compounds on the *P. falciparum* enzyme approaches

that of **1** and **2**. Activities against the enzyme and parasite correlate well, supporting the mode of action. Seven X-ray structures show that all of the new arylpropyl substituents displace a key tryptophan residue of the active-site flap, which had made favorable interactions with **1** and **2**. Plasticity of the flap allows substituents to be accommodated in many ways; in most cases, the flap is largely disordered. Compounds can be separated into two classes based on whether the substituent on the aromatic ring is at the *meta* or *para* position. Generally, *meta*-substituted compounds are better inhibitors, and in both classes, smaller size is linked to better potency.

Introduction

Despite major efforts to decrease its incidence in the last decade, malaria remains one of the leading causes of death from a single infectious agent. The disease, caused mostly by *Plasmodium falciparum*, was responsible for an estimated 438 000 deaths in 2015.^[1] Significant gains in recent years are being undermined by mounting resistance of the parasite to currently available drugs, so there is an urgent need for new chemical entities acting on new targets.

After Jomaa and co-workers demonstrated that *Plasmodia* synthesize isoprenoids via the non-mevalonate or 2-C-methyl-D-erythritol 4-phosphate (MEP) pathway,^[2] while humans obtain these essential molecules via the orthogonal mevalonate pathway,^[3,4] blocking the MEP pathway became an attractive strategy to stem the proliferation of this and other pathogens.^[5] 1-Deoxy-D-xylulose-5-phosphate reductoisomerase (Dxr; EC 1.1.1.267) catalyzes the first committed step in the MEP pathway, that is, the transformation of 1-deoxy-D-xylulose 5-phosphate (DOXP) to MEP.^[6,7] The natural antibiotic fosmidomycin (**1**, Figure 1), a potent inhibitor of Dxr,^[8,9] has been clinically evaluated for the treatment of malaria, alone and in combination therapy, but unfavorable pharmacokinetic properties and low intestinal absorption have prevented it from reaching the market.^[10–12] The acetyl homologue of fosmidomycin, FR-900098 (**2**), has been reported to be twice as potent against

[a] Dr. S. Sooriyaarachchi,[†] T. Bergfors, Dr. T. A. Jones, Dr. S. L. Mowbray[†] Science for Life Laboratory, Department of Cell and Molecular Biology, Uppsala University, Biomedical Center, Box 596, 751 24 Uppsala (Sweden)
E-mail: sherry.mowbray@icm.uu.se

[b] R. Chofor,[†] M. D. P. Risseeuw, Dr. S. Van Calenbergh[†] Laboratory for Medicinal Chemistry (FFW), Gent University, Ottergemsesteenweg 460, 9000 Gent (Belgium)
E-mail: serge.vancalenbergh@ugent.be

[c] Dr. J. Pouyez, Dr. J. Wouters
Department of Chemistry, University of Namur, Rue de Bruxelles 61, 5000 Namur (Belgium)

[d] Dr. C. S. Dowd
Department of Chemistry, George Washington University, Washington, DC 20052 (USA)

[e] Dr. L. Maes
Laboratory for Microbiology, Parasitology and Hygiene (LMPH), University of Antwerp, Universiteitsplein 1, 2610 Antwerp (Belgium)

[[†]] These authors contributed equally to this work.

Supporting information and the ORCID identification number(s) for the author(s) of this article can be found under <http://dx.doi.org/10.1002/cmdc.201600249>.

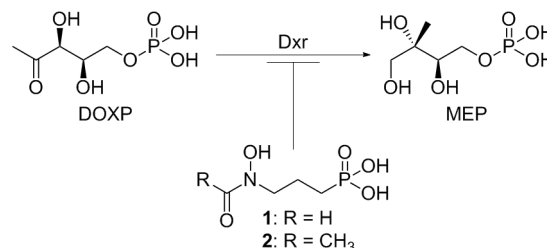


Figure 1. Conversion catalyzed by Dxr and two inhibitors of this enzyme.

P. falciparum in vitro, and against *P. vinckeii* in a mouse malaria model.^[2] Extensive medicinal chemistry efforts seeking new antimalarial agents have yielded various analogues of fosmidomycin, the subject of multiple reviews.^[13–15] The phosphonate group and the metal-chelating reverse hydroxamate moiety are both required for Dxr inhibitory activity. Aryl substitutions at the α -position (with respect to the phosphonate), when attached to the inhibitor backbone, have yielded some of the most promising analogues to date.

Dxr enzymes contain a strictly conserved tryptophan residue within a flexible loop (flap) that undergoes an induced-fit conformational change upon fosmidomycin binding, closing over and interacting with the bound inhibitor. This flap is considered essential for the catalytic activity of Dxr.^[16–20] Murkin and co-workers demonstrated a change in the rate-limiting step of the *Mycobacterium tuberculosis* Dxr-catalyzed reaction upon alteration of Trp203 in the flap, thereby establishing a functional link between this amino acid and chemical barrier crossing.^[21] Inhibition and binding studies with fosmidomycin confirmed the importance of the flap, and the conserved tryptophan in particular, for ligand binding. Structural evaluation of a series of Dxr-bound compounds including **3** and **4** (Figure 2) showed that the indole group of Trp211 in the *Escherichia coli* enzyme (EcDxr) is displaced in order to accommodate the inhibitors' pyridine/quinoline rings, which form π - π stacking or charge-transfer interactions with the indole of the tryptophan side chain.^[22]

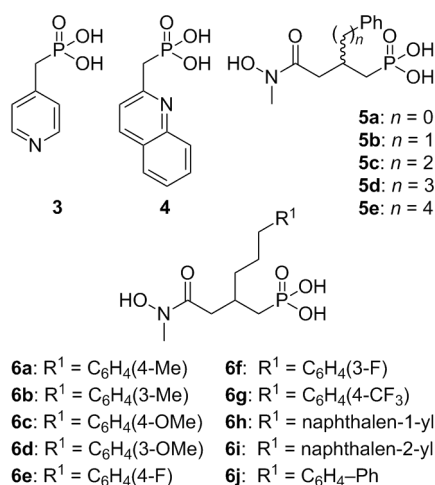


Figure 2. Relevant Dxr inhibitors **3–5** and target β -substituted fosmidomycin analogues **6a–j**.

Recently, we assessed the ability of Dxr to accommodate substituents in the β -position of fosmidomycin analogues bearing a hydroxamate rather than the original reverse hydroxamate group.^[23] We observed that direct introduction of aromatic rings at the β -carbon (as in **5a**) afforded moderate Dxr inhibitors. Exploration of different linkers between the β -carbon and a phenyl ring (**5b–e**) suggested that a 3-carbon linker (**5d**) was optimal for inhibition of EcDxr and *M. tuberculosis* Dxr, while both phenylpropyl (**5d**) and phenylbutyl (**5e**)

substituents afforded potent *P. falciparum* Dxr (PfDxr) inhibitors. These results were rationalized by crystallographic studies of PfDxr in complex with **5d** and **5e**, which showed that the phenyl rings of these compounds displace the indole ring of the conserved Trp296 residue, and occupy its 'usual' position in both active-site metal-containing^[16,18,24] and metal-free structures.^[17] This allows an intramolecular interaction between the phenyl ring and the methyl group on the hydroxamic acid that is equivalent to the intermolecular interactions observed in ternary complexes with **2**.^[18,24] Rearrangement of the residues of the flap results in favorable interactions between these phenyl rings and the tryptophan residue. Importantly, both analogues showed sub-micromolar schizontocidal activity against the *P. falciparum* K1 strain, and essentially the same SAR was observed as for PfDxr inhibition.

This follow-up study explored the influence of lipophilicity, electronic and steric properties in variants of the phenylpropyl side chain of **5d**. We anticipated that analogues **6a–j** would retain the capacity to occupy the aromatic 'hotspot', while their phenyl substituents might reinforce intra- or intermolecular interactions.

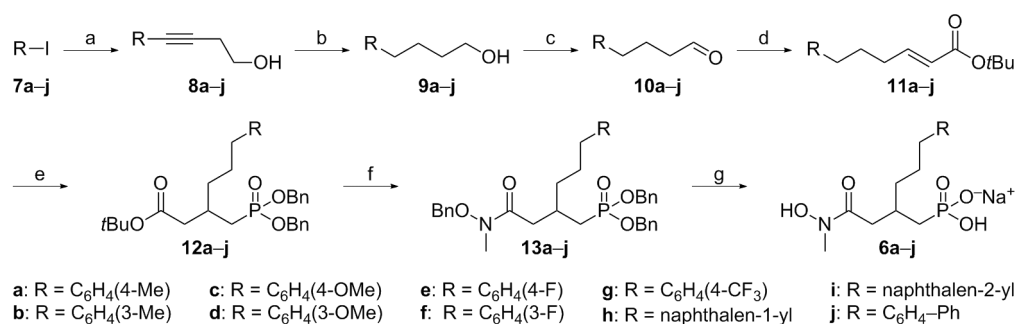
Results and Discussion

Synthesis

The synthesis of **6a–j** (Scheme 1) was achieved by starting from commercially available aryl iodides **7a–j**. Sonogashira coupling with but-3-yn-1-ol afforded the corresponding alkynols **8a–j**, which were readily converted into **9a–j** upon catalytic hydrogenation. Dess–Martin oxidation to the corresponding aldehydes **10a–j** and subsequent Wittig olefination afforded the α,β -unsaturated esters **11a–j**, which served as electrophiles in a Michael reaction with dibenzyl methylphosphonate to yield the 1,4-addition adducts **12a–j**. Hydrolysis of the *tert*-butyl ester and EDC mediated coupling with *O*-benzyl-*N*-methylhydroxylamine gave **13a–j**. Finally, removal of all benzyl protecting groups by catalytic hydrogenolysis afforded the desired analogues **6a–j**.

Evaluation of function

The final compounds were tested for inhibition of recombinant EcDxr and PfDxr using a spectrophotometric assay monitoring the substrate-dependent oxidation of NADPH associated with the Dxr-catalyzed reaction (Table 1).^[16,23,25] None of the changes introduced in **6a–6j** improve inhibition of EcDxr relative to **5d**, although **6a**, **6c**, **6d** and **6f** are essentially equipotent to **5d**. Two changes improve inhibition of PfDxr relative to **5d** (**6b** and **6f**), while three others give similar IC_{50} values (**6a**, **6c** and **6d**). The remaining changes are associated with weaker inhibition of PfDxr (**6e**, **6g–6j**). Surprisingly, methyl substitution of the aromatic ring at the *meta* position (**6b**) increases PfDxr inhibition, while it unfavorably influences EcDxr inhibition (Supporting Information (SI) Figure S1). The same may be true for the *meta*-fluoro analogue **6f**.



Scheme 1. Reagents and conditions: a) but-3-yn-1-ol, PdCl₂(PPh₃), CuI, Et₃N, 117 °C, 50–98%; b) H₂, Pd/C, MeOH, 69–94%; c) Dess–Martin periodinane, CH₂Cl₂; d) Ph₃P=CHCOOtBu, toluene, 120 °C, 49–67%; e) (BnO)₂OPMe, nBuLi, THF, –78 °C, 43–71%; f) 1. TFA, CH₂Cl₂, 45 min, 0 °C → RT; 2. MeN(OBn)H, EDC, DMAP, CH₂Cl₂, 18 h, RT, 44–78%; g) H₂, Pd/C, MeOH, NaOH_(aq), 25 °C, 10–15 min, quant.

Table 1. In vitro inhibition of recombinant Dxr enzymes, as well as growth of the *P. falciparum* K1 strain.

Compound	EcDxr ^[a]	IC ₅₀ [μM] PfDxr ^[a]	<i>P. fal.</i> K1 ^[b]
	ND ^[c]	0.036 (0.032–0.040)	1.7 ± 0.9 ^[26]
	0.03 (0.02–0.05) ^[d]	0.045 (0.041–0.049) ^[d]	0.4 ± 0.2 ^[26]
	0.84 ^[23] (0.51–1.40)	0.079 (0.066–0.093) ^[e]	2.7 ± 0.1 ^[f]
	1.04 (0.6–1.8)	0.175 (0.129–0.237)	1.4 ± 1.2
	10.40 (2.8–388.3)	0.05 (0.043–0.049)	10.9 ± 4.5
	1.18 (0.4–3.3)	0.12 (0.096–0.142)	3.8 ± 2.5
	0.97 (0.62–1.5)	0.15 (0.137–0.154)	7.8 ± 3.7

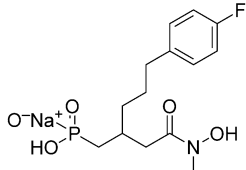
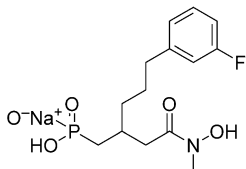
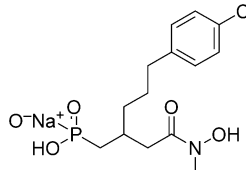
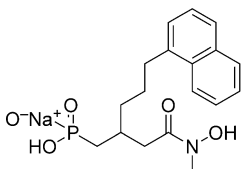
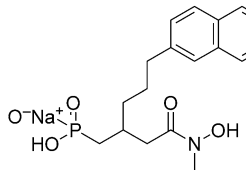
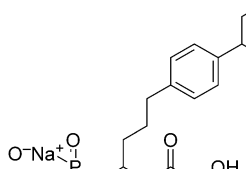
None of the changes introduced in **6a–6j** relative to **5d** significantly improve the IC₅₀ values regarding in vitro growth of the multidrug-resistant *P. falciparum* K1 strain (Table 1). However, improvement of IC₅₀ for PfDxr is well correlated with improvements in the IC₅₀ against the parasite (Figure 3), indicating that Dxr is in fact the primary target of this series of compounds. Only inhibitors with IC₅₀ values better than ~0.3 μM (pIC₅₀ greater than 6.5) had significant effects against the parasite at the highest concentration tested (64 μM).

Results against *Trypanosoma brucei brucei* Squib 427, *T. cruzi* Tulahuen LacZ (clone C4) and *Leishmania infantum* MHOM/MA(BE)/67 strains were also negative at the highest concentrations tested (64 μM).^[29] Because these parasites do not have Dxr, these were effectively control experiments. Cytotoxicity, as assessed against MRC-5_{SV2} (human lung fibroblast) cells, was also negligible for all compounds at this concentration.

X-ray crystal structures of PfDxr in complex with seven inhibitors

The structures of PfDxr in complex with seven of the new β-substituted inhibitors (**6a–d**, **6f**, **6g**, **6h**) are described in more detail in the Supporting Information. Although all of the new compounds were entered into crystallization trials, only inhibitors with IC₅₀ values better than ~0.5 μM (pIC₅₀ greater than ~6.2) produced structures (Figures 3–5). The structures have been solved at resolutions in the range of 1.4–1.8 Å, and refined to crystallographic *R*-factors of ~18% and free *R*-factors of 20–21%. Complete data collection and refinement statistics are given in SI Table S2. Each complex has been crystallized in space group P1, with similar unit cell constants. A dimer is found in the asymmetric unit, and a manganese ion and an inhibitor molecule are very clear in each active site (Figure 4a). The overall electron density is of good quality, and complete models of the enzyme

Table 1. (Continued)

Compound	EcDxr ^[a]	IC ₅₀ [μM] PfDxr ^[a]	<i>P. fal.</i> K1 ^[b]
6e 	10.53 (2.4–46.2)	3.2 (2.83–3.63)	51.4 ± 21.8
6f 	2.00 (1.1–3.7)	0.067 (0.057–0.078)	5.7 ± 4.4
6g 	7.33 (0.9–59.6)	0.27 (0.248–0.295)	45.7 ± 21.3
6h 	13.91 (4.3–45.5)	0.28 (0.272–0.298)	49.3 ± 18.9
6i 	4.07 (1.5–11.2)	0.87 (0.780–0.977)	46.6 ± 15.4
6j 	ND ^[g]	1.6 (1.16–2.158)	> 64

[a] IC₅₀ values reported for EcDxr were calculated from a single curve, whereas those for PfDxr are based on three experiments (the confidence interval for each value is shown in parentheses). [b] IC₅₀ values for *Plasmodium* growth are the mean ± SD of three separate experiments performed on different dates. [c] Not determined; a value of 0.030 ± 0.008 was reported earlier.^[27] [d] Values of 0.051 and 0.018 were reported earlier for EcDxr and PfDxr, respectively.^[28] [e] A value of 0.117 ± 0.012 was reported earlier.^[23] [f] A value of 0.43 ± 0.09 was reported earlier.^[23] [g] Not determined; 86% activity remained after the addition of 100 μM **6j**.

are deposited at the PDB for residues 77–486 in each chain. However, the electron density for even the main chain in some of the flap (residues 292–298) is sometimes poorly defined; see SI Table S3. Only in the complex with **6h**, and in one molecule of **6d**, is the main-chain electron density of each flap continuous at the RMS value of the relevant map. The indole ring of Trp296 is poorly defined in six of the 14 views of the active site. Although each compound was synthesized as a racemic mixture, the high resolution of the structures allowed us to

identify the favored *R*-enantiomer in each complex, as observed in our earlier work.^[23] The protein structures are highly conserved; a structural superposition of each chain onto the A chain of the **5d** complex (PDB ID: 4Y67) produces RMS values of 0.16–0.36 Å for 398–410 pairs of C α atoms, when using a 1 Å C α -pair cutoff. The overlapping C α -traces show separation into A and B chain clusters at the start of two helices in the cofactor-binding domain, probably as a result of differences in the crystal environment. Because the electron density in the flap is often poorly defined, the chains are not tightly clustered, but short regions before and after the flap show separate tight A- and B-chain clusters, again separated by ~0.5–1.0 Å, probably as a result of different crystal contacts.

There is no clear correlation between strength of inhibition and temperature factors or fit to electron density (SI Figure S2), which is perhaps to be expected given the variable conformations observed for the flap.

Numerous crystallographic studies have shown that fosmidomycin analogues bind in the substrate/product-binding site of Dxr. The phosphonate group at one end is held firmly in place by multiple hydrogen-bonding interactions with protein and solvent, and the hydroxamic acid group at the other end is coordinated to the active-site metal ion. In ternary complexes with **1** and **2**, a well-defined flap has been observed, with a number of highly conserved amino acid side chains contributing to the binding site.^[16–18,24] In particular, the indole ring of Trp296 (PfDxr numbering) packs against the backbone of the two compounds, and interacts with the methyl group of the acetyl derivative **2**.^[16,18,24] In the numerous structures with α -aryl analogues, the flap is either disordered or has moved to allow the substituents to bind in a depression located between three ordered loops and a usually disordered flap. This depression is large enough to accommodate analogues with formyl, acetyl or phenyl substituents at the hydroxamate group, for example.^[31–33] β -aryl substituents, however, show at least two modes of binding.^[23] For the **5a** complex that lacks a linker, the phenyl group is positioned ‘under’ a well-defined flap, and the methyl group on the hydroxamic acid interacts with the indole ring of Trp296. For the **5d** and **5e** complexes, however, the linkers adopt boomerang-like conformations that, together with small changes in the fosmidomycin backbone, allow their respective phenyl groups to interact with the methyl group of their hydroxamic acid. In this strikingly different way of dealing with the substitution, the linker occupies the volume normally occupied by α -aryl substitutions, while the phenyl ring is co-spatial with the indole ring of the flap tryptophan, as seen in ternary complexes.^[16–18,24] The edge of the phenyl ring, in turn, interacts with the indole ring of Trp296 in the flap. All seven of the new

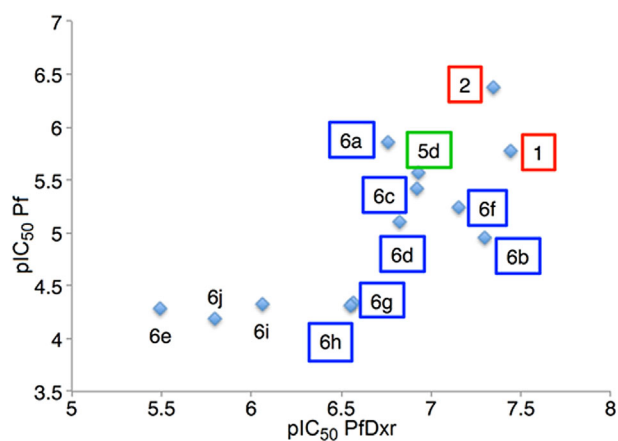


Figure 3. Plot of pIC_{50} against in vitro growth of the *P. falciparum* K1 strain versus pIC_{50} against PfDxr activity for the new compounds; data for **1** and **2** are shown for reference. Compounds marked with blue boxes are those for which X-ray structures of complexes with PfDxr are reported herein, whereas red^[18] and green^[23] boxes indicate structures reported elsewhere.

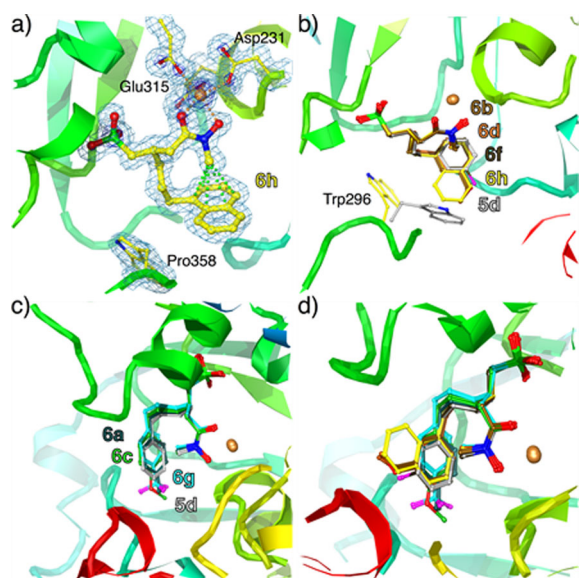


Figure 4. X-ray structures of PfDxr in complex with inhibitors. The cartoon representation of the protein backbone is color coded according to position in the sequence, going through the rainbow from red to blue. a) Electron density for the inhibitor **6h** and selected nearby atoms, contoured at the RMS value of the σ_A -weighted ($2m|F_o| - D|F_c|$) electron-density map^[30] (0.43 e \AA^{-3}) in light blue, as well as at 2.5 e \AA^{-3} (gold) to show the higher electron density near the metal ion. b) Superimposed structures of the *meta*-class compounds, **6b** (light brown), **6d** (orange), **6f** (dark brown) and **6h** (yellow), on **5d** (silver gray). The well-defined flap residue, Trp296, of **6h** and **5d** is observed to undergo a conformational change. c) Superimposed structures of the *para*-class compounds, **6a** (dark green), **6c** (light green) and **6g** (cyan), on **5d** (silver gray). Fluorine atoms are shown in magenta. d) All the structures superimposed, using the same coloring scheme defined in panels b and c.

β -substituted complexes take on the same general structure observed in the **5d** complex, but can be grouped into two sets depending on whether they represent *meta* or *para* substitutions to the phenyl ring. We have structures for three *meta* (**6b**, **6d**, **6f**) and three *para* (**6a**, **6c**, **6g**) substitutions,

as well as **6h**, which we consider as a member of the *meta* class.

The members of the *meta* class form a tight cluster of eight independent structures (including both subunits of the dimers), where the phenyl rings of the new compounds closely overlap that observed in the **5d** complex (Figure 4b). Interactions of the phosphonate and hydroxamic acid groups in all complexes are essentially identical to those of the **5d** complex,^[23] as is the overall conformation of the fosmidomycin backbone. All members adopt the same pose, where the substituent is directed toward the indole ring of Trp296 in the **5d** complex; none points in the other direction, toward His341. However, all inhibitors have an effect on the positioning of the indole ring, and on the quality of the electron density of the flap (SI Table S3). Unsurprisingly, the introduction of a naphthalene ring in **6h** causes a large change in the conformation of Trp296, which is needed to prevent clashes (Figure 4b); the flap in this structure is well defined. Although there are no close contacts to the indole ring, only a few atoms of one edge of the naphthalene ring are solvent-exposed. The slightly smaller methoxyphenyl substituent in **6d** causes a different movement of the tryptophan residue, needed to prevent close contacts between the indole ring and the methyl group. The flap is rather well defined in both chains, as is the density for the indole group, but the change in conformation results in a loss of the close contacts to the indole seen in the **5d** complex. The methoxyphenyl group is approximately planar, and so occupies the same place as the corresponding portion of the naphthalene ring of **6h** (Figure 4b). The methoxy group does not form any hydrogen-bonding interactions with the protein, and is shielded from the solvent by residues near 360. The introduction of the methyl and fluorine substituents in **6b** and **6f**, respectively, would result in close contacts to one edge of the indole, if the conformation seen in the **5d** complex were maintained (three contacts are predicted, of 2.5 \AA and $\sim 3.1 \text{ \AA}$, in **6b** and **6f**, respectively). Instead, the flap moves, and the electron density in a three-residue segment of the flap (residues 294–296) becomes poorly defined (SI Table S3); the indole ring is moderately clear in only one of the four active sites (that of the **6f** A-chain). Compounds **6b** and **6f** show equal or better IC_{50} values than **5d**, however, while the other two *meta* compounds have higher values (Figure 3 and Table 1). The lack of well-defined interactions between the best inhibitors and the indole ring of Trp296 suggests that the interactions with the indole that are observed in the **5d** complex are not the most important determinants of the observed IC_{50} values. However, it is striking that the larger the substituent, the higher the IC_{50} observed (Figure 5a). We suggest that the most energetically favorable intramolecular phenyl/methyl interactions are harder for inhibitors with larger substituents to attain in the complexes, because they occur in the context of enzyme–inhibitor interactions.

The members of the *para* group (**6a**, **6c**, **6g**) form a cluster of six similar structures that are distinct from those of the *meta* group (Figure 4c). The interactions at the phosphonate and hydroxamic acid moieties are essentially identical in all complexes, as is the conformation of the fosmidomycin backbone.

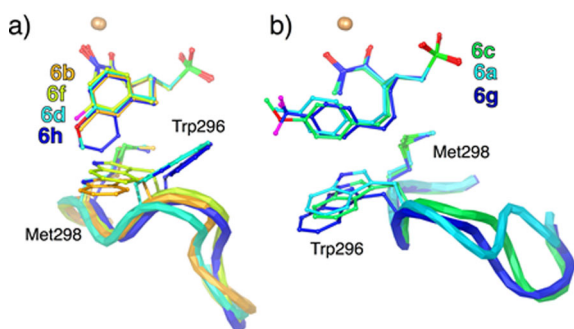


Figure 5. Relationship between substituent size and $pI_{C_{50}}$. The inhibitors and residues of their respective flaps are colored on a common scale, going through the rainbow from the best $pI_{C_{50}}$ value (red, using **1** as the endpoint) to the poorest (blue). a) Complexes of the *meta* cluster: it should be remembered that the **6b** complex, in particular, has poor electron density for the indole of Trp296. b) Complexes of the *para* cluster: note that the **6g** complex has no significant electron density in the flap, as well as weaker electron density in the three-carbon linker of the inhibitor.

While their phenyl rings are closely co-planar with that of the **5d** complex, the rings are not so tightly clustered and each is shifted to some degree within the binding site by virtue of the flexible 3-carbon linker. The smallest shift from **5d** is associated with the smallest substitution, and so on: ~ 0.5 Å for **6a**, ~ 0.7 Å for **6c** and ~ 1.0 Å for **6g**. This results from steric constraints near Met360/Pro363 that “push” the larger substituents away. Small differences in the torsion angles give the effect of splaying the linker, while sliding the ring in the plane of the phenyl ring seen in **5d** (Figure 4c). The important intra-ligand ring-methyl group interactions are, therefore, maintained in all complexes, but with variations (Figure 4d). Again, the electron density in each complex is poorly defined in regions of the flap; the indole ring of Trp296 is well defined in only three active sites; see SI Table S3. In these three complexes, Trp296 is similar to the **5d** complex, and the indole ring helps to shield the edge of the phenyl ring of the inhibitor. However, the tryptophan is not forced out of the active site, as was observed for the largest *meta*-group compounds. Two of the fluorine atoms in **6g** interact with a water molecule that is highly conserved in the various structures (although slightly displaced in the **6a** complex), while the oxygen atom in the methoxy-substituent of **6c** accepts a hydrogen bond from the main-chain amide nitrogen of residue 359. In general, the larger the *para*-group substituent, the poorer the IC_{50} (Figure 5b). This is probably due to the translation of the relevant phenyl group from its energetically-preferred position in the **5d** complex, although this is compensated for in part by interactions of **6g** and **6c** with structurally-conserved polar atoms. Overall, the *para*-substituted ligands are poorer inhibitors than their *meta* equivalents (placing **6i** in the *para* group, as the *para* equivalent of **6h**).

Conclusions

In the present work, we continued our systematic study of β -substituted hydroxamate analogues of fosmidomycin. Specifically, we explored the effects of changes in lipophilicity, elec-

tronic and steric properties versus the phenylpropyl side chain of the earlier compound **5d**. Several of the new compounds exhibit potency on PfDxr that approaches that of **1** and **2**. There is a good correlation between activity against the enzyme, and activity against the parasite, indicating that their primary mode of biological action is in fact via PfDxr. Seven new X-ray structures show that all of the new arylpropyl substituents displace the key tryptophan residue of the active-site flap, which had made favorable interactions with the reverse hydroxamate group of **1** and its acetyl homologue **2**. The plasticity of the flap allows the various compounds to be accommodated in many ways, and indeed in most cases, the flap is largely disordered. However, the results can be separated into two groups, based on whether the substituent on the aromatic ring is *meta* or *para*. Generally, *meta* compounds are better inhibitors, and in both classes smaller substituents are associated with better potency. The large lipophilic biphenyl and naphthyl substituents provided poor inhibitors of Dxr, which was not compensated for by any advantages such compounds might provide regarding entry into the parasite cell and apicoplast, or other factors. Future directions should include tests of additional small substituents, particularly those that could make good interactions with one of the favored conformations of the enzyme. However, it remains to be seen whether intestinal absorption, pharmacokinetic properties or other properties are improved for any of the β -arylpropyl analogues. The strength of the present study is that it provides multiple viable compounds for additional biological work, increasing the chances of ultimate success in the effort to develop useful drugs of the fosmidomycin class.

Experimental Section

General: All reactions described were performed under an argon atmosphere and at ambient temperature unless stated otherwise. All reagents and solvents were purchased from Sigma-Aldrich (Diegem, Belgium), Acros Organics (Geel Belgium), or TCI Europe (Zwijndrecht, Belgium) and used as received (except THF). Tetrahydrofuran was dried over sodium/benzophenone. NMR solvents were purchased from Eurisotop (Saint Aubin, France). Reactions were monitored by TLC analysis using TLC aluminum sheets (Macherey-Nagel, Alugram Sil G/UV₂₅₄). Detection was observed by spraying with a solution of $(NH_4)_6Mo_7O_{24} \cdot 4H_2O$ (25 g L^{-1}) and $(NH_4)_4Ce(SO_4)_4 \cdot 2H_2O$ (10 g L^{-1}) in H_2SO_4 (10%) followed by charring or immersion in an aqueous solution of $KMnO_7$ (20 g L^{-1}) and K_2CO_3 (10 g L^{-1}) or an ethanolic solution of ninhydrin (2 g L^{-1}) and acetic acid (1% v/v) followed by charring. Silica gel column chromatography was performed manually using Grace Davisil 60 Å silica gel (40–63 μm) or automated using a Grace Reveleris X2 system and the corresponding flash cartridges. High-resolution spectra were recorded with a Waters LCT Premier XE Mass spectrometer. 1H and ^{13}C NMR spectra were recorded with a Varian Mercury 300BB (300/75 MHz) spectrometer. Chemical shifts are given in ppm (δ) relative to tetramethylsilane (1H NMR) or the NMR solvent (^{13}C NMR) as an internal standard. In ^{31}P NMR, signals are referenced to the $CDCl_3$ or D_2O lock resonance frequency according to IUPAC referencing, with H_3PO_4 set to 0.00 ppm. Coupling constants are given in Hz. Preparative HPLC purifications were carried out using a Laprep preparative HPLC system equipped with an Xbridge

Prep C₁₈ column (19×250 mm, 5 μm) using a H₂O/CH₃CN/HCOOH gradient solvent system. All synthesized compounds were ≥95% pure as verified by LC–MS.

General procedure I: Sonogashira coupling toward aralkynols 8a–j: To a solution of the aryl iodides 7a–j in degassed Et₃N was added PdCl₂(PPh₃)₂, CuI and but-3-yn-1-ol. The reaction mixture was held at reflux at 117 °C for 3 h, after which it was cooled and concentrated in vacuo. Column chromatography using a hexane/EtOAc solvent system afforded compounds 8a–j.

General procedure II: triple bond reduction: To a solution of the alkynes 8a–j in MeOH, was added 10% Pd/C under a nitrogen atmosphere. Molecular hydrogen (H₂) was bubbled through the mixture for 30 min followed by filtration through a Whatman filter paper path. In vacuo concentration yielded compounds 9a–j, which were used for the next step without further purification.

General procedure III: Dess–Martin oxidation and concomitant Wittig olefination: A solution of the starting materials (9a–j) in CH₂Cl₂ and a nitrogen atmosphere was cooled to 0 °C. Dess–Martin periodinane (2.0 equiv) was added, and the mixture was allowed to warm to RT. After stirring for 3 h, TLC analysis showed a completed reaction. The reaction mixture was washed once with a 5:1 mixture of NaHCO₃ (sat. aq.) and Na₂S₂O₃ (aq. 2.0 M), and the aqueous layer was extracted three times with Et₂O. The combined organic layer was washed successively with a 0.1 M solution of HCl and brine, dried over anhydrous Na₂SO₄ and concentrated in vacuo to obtain the corresponding aldehydes (10a–j) which was used without further purification. The aldehyde was dissolved in toluene under nitrogen atmosphere and *tert*-butyl(triphenylphosphoranylidene)acetate (3 equiv) was added. An overnight reflux at 120 °C was followed by cooling and in vacuo concentration. Sorption of the crude on Celite and silica gel chromatography gave access to the *tert*-butyl esters 11a–j.

General procedure IV: Michael addition of methylphosphonate diesters to α,β-unsaturated *tert*-butyl esters: To a solution of dibenzylmethyl phosphonate (2 equiv) in THF and under a nitrogen atmosphere was added *n*BuLi (2 equiv) at –78 °C. After 30 min, a solution of the ester was added to the reaction mixture dropwise. Three hours later, the reaction was shown to be complete by TLC and was quenched with NH₄Cl (sat. aq.). The aqueous layer was extracted three times with EtOAc. Organic fractions were pooled, washed once with brine and dried over anhydrous Na₂SO₄. Column chromatography (hexane/EtOAc system) afforded the adducts 12a–j.

General procedure V: acidic cleavage of the *tert*-butyl ester and protected hydroxamate formation: A 0.1 M solution of the starting materials (12a–j) in CH₂Cl₂/TFA (80:20) at 0 °C was stirred for 2 h, after which excess toluene was added to the reaction mixture and concentrated in vacuo. The crude acid was re-dissolved in CH₂Cl₂ (0.1 M), followed by addition of EDC (1.2 equiv), DMAP (1.2 equiv), and Et₃N (2.0 equiv). *O*-Benzyl-*N*-methylhydroxylamine TFA salt (1.2 equiv) was added as a 0.2 M solution in CH₂Cl₂, and the mixture was stirred overnight at RT. The reaction was subsequently quenched with sat. aq. NaHCO₃, extracted three times with CH₂Cl₂, washed with brine and dried over Na₂SO₄. Column chromatography (CH₂Cl₂/MeOH system) produced the protected hydroxamic acids to yield compounds 13a–j.

General procedure VI: catalytic hydrogenolysis of benzyl protective groups: The benzyl-protected compounds 13a–j (100–130 mg) were dissolved in MeOH (10 mL) under an inert atmosphere and 10% Pd/C was added. The resulting mixture was then

stirred under hydrogen atmosphere while monitoring the progress by mass spectrometry. At completion (~10 min), the reaction mixture was filtered and neutralized with NaOH (1 equiv). The reaction mixture was then concentrated in vacuo, re-dissolved in a 1:1 (v/v) mixture of H₂O and *t*BuOH, frozen and lyophilized to afford the desired targets compounds 6a–j as monosodium phosphonic acid salts in quantitative yield.

***tert*-Butyl (E)-6-(*p*-tolyl)hex-2-enoate (11 a):** Prepared according to general procedure III. Purification 1:1 toluene/hexane v/v; yield 59%; colorless oil. ¹H NMR (300 MHz, CDCl₃): δ_H=1.47 (brs, 9H, *t*Bu), 1.75 (app quint, *J*=8.0 Hz, 2H, –CH₂–), 2.12–2.23 (m, 2H, –CH₂–), 2.30 (s, 3H, Ph-CH₃), 2.58 (t, *J*=7.5 Hz, 2H, –CH₂–), 5.74 (dt, *J*=1.5 Hz, 15.6 Hz, 1H, –CH=CHCO), 6.87 (dt *J*=7.1 Hz, 15.6 Hz, 1H, –CH=CHCO), 7.00–7.16 ppm (m, 4H, Ar-H); ¹³C NMR (75 MHz, CDCl₃): δ_C=20.9, 28.1, 29.7, 31.4, 34.7, 79.9, 123.2, 128.2, 128.9, 135.2, 138.6, 147.5, 170.0 ppm; HRMS (ESI): calcd for C₁₇H₂₅O₂ [M+H]⁺: 261.1849, found: 261.1856.

***tert*-Butyl (E)-6-(*m*-tolyl)hex-2-enoate (11 b):** Prepared according to general procedure III. Purification 1:1 toluene/hexane v/v; yield 51%; colorless oil. ¹H NMR (300 MHz, CDCl₃): δ_H=1.44 (brs, 9H, *t*Bu), 1.76 (app quint, *J*=7.7 Hz, 2H, –CH₂–), 2.14–2.24 (m, 2H, –CH₂–), 2.32 (s, 3H, Ph-CH₃), 2.59 (t, *J*=7.7 Hz, 2H, –CH₂–), 5.75 (dt, *J*=1.6 Hz, 15.6 Hz, 1H, –CH=CHCO), 6.87 (dt *J*=6.9 Hz, 15.5 Hz, 1H, –CH=CHCO), 6.93–7.02 (m, 3H Ar-H), 7.12–7.20 ppm (m, 1H, Ar-H); ¹³C NMR (75 MHz, CDCl₃): δ_C=21.3, 28.1, 29.7, 31.5, 35.2, 80.0, 123.3, 125.4, 126.6, 128.2, 129.2, 137.8, 141.7, 147.5, 166.0 ppm; HRMS (ESI): calcd for C₁₇H₂₅O₂ [M+H]⁺: 261.1849, found: 261.1852.

***tert*-Butyl (E)-6-(4-methoxyphenyl)hex-2-enoate (11 c):** Prepared according to general procedure III. Purification 1:1 toluene/hexane v/v; yield 64%; white wax. ¹H NMR (300 MHz, CDCl₃): δ_H=1.47 (brs, 9H, *t*Bu), 1.73 (app quint, *J*=7.7 Hz, 2H, –CH₂–), 2.12–2.23 (m, 2H, –CH₂–), 2.32 (s, 3H, Ph-CH₃), 2.57 (t, *J*=7.4 Hz, 2H, –CH₂–), 3.76 (s, 3H, PhOCH₃), 5.74 (dt, *J*=1.7 Hz, 15.7 Hz, 1H, –CH=CHCO), 6.82 (dt *J*=6.4 Hz, 15.7 Hz, 1H, –CH=CHCO), 7.26–7.42 ppm (m, 4H, Ar-H); ¹³C NMR (75 MHz, CDCl₃): δ_C=28.1, 29.8, 31.3, 34.2, 55.1, 78.3, 113.7, 123.2, 129.2, 133.7, 147.5, 157.7, 166.0 ppm; HRMS (ESI): calcd for C₁₇H₂₅O₃ [M+H]⁺: 277.1798, found: 277.1790.

***tert*-Butyl (E)-6-(3-methoxyphenyl)hex-2-enoate (11 d):** Prepared according to general procedure III. Purification 1:1 toluene/hexane v/v; yield 65%; white viscous oil. ¹H NMR (300 MHz, CDCl₃): δ_H=1.46 (brs, 9H, *t*Bu), 1.76 (app quint, *J*=7.6 Hz, 2H, –CH₂–), 2.16–2.24 (m, 2H, –CH₂–), 2.57 (t, *J*=7.6 Hz, 2H, –CH₂–), 3.72 (s, 3H, PhOCH₃), 5.73 (dt, *J*=1.6 Hz, 15.7 Hz, 1H, –CH=CHCO), 6.87 (dt *J*=6.9 Hz, 15.7 Hz, 1H, –CH=CHCO), 6.92–7.04 (m, 3H Ar-H), 7.12–7.21 ppm (m, 1H, Ar-H); ¹³C NMR (75 MHz, CDCl₃): δ_C=27.9, 28.1, 29.4, 31.5, 35.8, 80.0, 123.3, 125.4, 126.6, 128.2, 129.2, 137.8, 141.7, 146.8, 165.4 ppm; HRMS (ESI): calcd for C₁₇H₂₅O₃ [M+H]⁺: 277.1798, found: 277.1799.

***tert*-Butyl (E)-6-(4-fluorophenyl)hex-2-enoate (11 e):** Prepared according to general procedure III. Purification 1:1 toluene/hexane v/v; yield 53%; pale-yellow oil. ¹H NMR (300 MHz, CDCl₃): δ_H=1.47 (brs, 9H, *t*Bu), 1.66–1.82 (app quint, *J*=7.6 Hz, 2H, –CH₂–), 2.19 (m, 2H, –CH₂–), 2.60 (t, *J*=7.4 Hz, 2H, –CH₂–), 5.75 (dt, *J*=1.7 Hz, 15.80 Hz, 1H, –CH=CHCO), 6.80–7.00 (m, 3H, –CH=CHCO, Ar-H), 7.06–7.15 ppm (m, 2H, Ar-H); ¹³C NMR (75 MHz, CDCl₃): δ_C=28.1, 29.8, 31.3, 34.4, 80.0, 115.0 (d, ²J_{C-F}=20.9 Hz), 123.4, 129.7 (d, ³J_{C-F}=8.8 Hz), 137.3 (d, ⁴J_{C-F}=3.6 Hz), 147.2, 161.3 (d, ¹J_{C-F}=242.9 Hz), 166.0 ppm; HRMS (ESI): calcd for C₁₆H₂₂FO₂ [M+H]⁺: 265.1598, found: 265.1597.

tert-Butyl (E)-6-(3-fluorophenyl)hex-2-enoate (11 f): Prepared according to general procedure III. Purification 1:1 toluene/hexane *v/v*; yield 49%; pale-yellow oil. ¹H NMR (300 MHz, CDCl₃): δ_H = 1.48 (brs, 9H, tBu), 1.78 (app quint, *J* = 8.0 Hz, 2H, -CH₂-), 2.15–2.25 (m, 2H, -CH₂-), 2.63 (t, *J* = 7.7 Hz, 2H, -CH₂-), 5.75 (dt, *J* = 1.7 Hz, 15.6 Hz, 1H, -CH=CHCO), 6.79–6.97 (m, 4H, -CH=CHCO, Ar-H), 7.18–7.27 ppm (m, 1H, Ar-H); ¹³C NMR (75 MHz, CDCl₃): δ_C = 28.1, 29.4, 31.3, 34.9 (d, ⁴*J*_{C-F} = 1.8 Hz), 80.1, 112.7, 115.2 (d, ²*J*_{C-F} = 21.1 Hz), 123.5, 124.0 (d, ⁴*J*_{C-F} = 2.8 Hz), 129.7 (d, ³*J*_{C-F} = 8.2 Hz), 144.3 (d, ³*J*_{C-F} = 7.1 Hz), 147.1, 162.8 (d, ²*J*_{C-F} = 245.5 Hz), 166.0 ppm; HRMS (ESI): calcd for C₁₆H₂₂FO₂ [*M* + *H*]⁺: 265.1598, found: 265.1599.

tert-Butyl (E)-6-(4-(trifluoromethyl)phenyl)hex-2-enoate (11 g): Prepared according to general procedure III. Purification 1:1 toluene/hexane *v/v*; yield 60%; colorless oil. ¹H NMR (300 MHz, CDCl₃): δ_H = 1.48 (brs, 9H, tBu), 1.80 (app quint, *J* = 7.5 Hz, 2H, -CH₂-), 2.21 (m, 2H, -CH₂-), 2.69 (t, *J* = 7.8 Hz, -CH₂-), 5.76 (dt, *J* = 1.8 Hz, 15.6 Hz, 1H, -CH=CHCO), 6.86 (dt, *J* = 6.8 Hz, 15.6 Hz, 1H, -CH=CHCO), 7.28 (d, *J* = 9.0 Hz, 2H, Ar-H), 7.54 ppm (d, *J* = 8.5 Hz, 2H, Ar-H); ¹³C NMR (75 MHz, CDCl₃): δ_C = 28.1, 29.4, 31.3, 35.0, 80.1, 123.6, 124.3 (q, ¹*J*_{C-F} = 271.9 Hz), 125.3 (q, ³*J*_{C-F} = 7.2 Hz), 128.3 (q, ²*J*_{C-F} = 32.5 Hz), 128.7, 145.9, 146.9, 165.9 ppm; HRMS (ESI): calcd for C₁₇H₂₂F₃O₂ [*M* + *H*]⁺: 315.1566, found: 315.1570.

tert-Butyl (E)-6-(naphthalen-1-yl)hex-2-enoate (11 h): Prepared according to general procedure III. Purification 1:1 toluene/hexane *v/v*; yield 67%; colorless oil. ¹H NMR (300 MHz, CDCl₃): δ_H = 1.47 (brs, 9H, tBu), 1.90 (app quint, *J* = 7.6 Hz, 2H, -CH₂-), 2.21–2.31 (m, 2H, -CH₂-), 3.08 (t, *J* = 7.6 Hz, -CH₂-), 5.78 (dt, *J* = 1.5 Hz, 15.6 Hz, 1H, -CH=CHCO), 6.91 (dt, *J* = 6.9 Hz, 15.6 Hz, 1H, -CH=CHCO), 7.26–7.53 (m, 4H, Ar-H), 7.70 (d, *J* = 8.4 Hz, 1H, Ar-H), 7.80–8.00 ppm (m, 2H, Ar-H); ¹³C NMR (75 MHz, CDCl₃): δ_C = 28.1, 28.9, 31.8, 32.4, 80.0, 123.4, 123.6, 125.4, 125.5, 125.7, 126.0, 126.7, 128.7, 131.7, 133.9, 137.8, 147.3, 166.0 ppm; HRMS (ESI): calcd for C₂₀H₂₅O₂ [*M* + *H*]⁺: 297.1849, found 297.1854.

tert-Butyl (E)-6-(naphthalen-2-yl)hex-2-enoate (11 i): Prepared according to general procedure III. Purification 1:1 toluene/hexane *v/v*; yield 67%; colorless oil. ¹H NMR (300 MHz, CDCl₃): δ_H = 1.48 (brs, 9H, tBu), 1.84 (app quint, *J* = 8.1 Hz, 2H, -CH₂-), 2.21 (m, 2H, -CH₂-), 2.77 (t, *J* = 7.7 Hz, -CH₂-), 5.76 (dt, *J* = 1.6 Hz, 15.2 Hz, 1H, -CH=CHCO), 6.89 (dt, *J* = 7.3 Hz, 15.8 Hz, 1H, -CH=CHCO), 7.29 (dd, *J* = 1.8 Hz, 8.4 Hz, 1H, Ar-H), 7.36–7.47 (m, 2H, Ar-H), 7.58 (s, 1H, Ar-H), 7.71–7.81 ppm (m, 2H, Ar-H); ¹³C NMR (75 MHz, CDCl₃): δ_C = 28.1, 29.5, 31.4, 35.3, 80.0, 123.3, 125.1, 125.8, 126.4, 127.1, 127.3, 127.5, 127.9, 132.0, 133.5, 139.2, 147.4, 166.0 ppm; HRMS (ESI): calcd for C₂₀H₂₅O₂ [*M* + *H*]⁺: 297.1849, found: 297.1852.

tert-Butyl (E)-6-([1,1'-biphenyl]-4-yl)hex-2-enoate (11 j): Prepared according to general procedure III. Purification 1:1 toluene/hexane *v/v*; yield 61%; brown oil. ¹H NMR (300 MHz, CDCl₃): δ_H = 1.48 (brs, 9H, tBu), 1.84 (app quint, *J* = 7.5 Hz, 2H, -CH₂-), 2.21–2.35 (m, 2H, -CH₂-), 2.65 (t, *J* = 7.8 Hz, -CH₂-), 5.75 (dt, *J* = 1.7 Hz, 15.7 Hz, 1H, -CH=CHCO), 6.90 (dt, *J* = 6.8 Hz, 15.7 Hz, 1H, -CH=CHCO), 7.22 (d, *J* = 8.5 Hz, 2H, Ar-H), 7.27–7.67 ppm (m, 7H, Ar-H); ¹³C NMR (75 MHz, CDCl₃): δ_C = 28.1, 29.6, 31.4, 34.8, 80.0, 123.4, 126.9, 127.0, 127.1, 128.7, 128.8, 138.8, 140.8, 141.0, 147.4, 166.0 ppm; HRMS (ESI): calcd for C₂₂H₂₇O₂ [*M* + *H*]⁺: 323.2006, mass not found.

tert-Butyl 3-((bis(benzyloxy)phosphoryl)methyl)-6-(*p*-tolyl)hexanoate (12 a): Prepared according to general procedure IV. Purification 2:1 hexane/EtOAc *v/v*; yield 54%; colorless oil. ¹H NMR (300 MHz, CDCl₃): δ_H = 1.38 (brs, 9H, tBu), 1.42–1.62 (m, 4H, -CH₂-), 1.76–1.95 (m, 2H, -CH₂-), 2.19–2.32 (m, 5H, Ph-CH₃, -CH₂-), 2.35–2.54 (m, 3H, -CH₂-, -CH-), 4.87–5.08 (m, 4H, -CH₂-Ph), 6.97–7.08 (m, 4H, Ar-H), 7.28–7.35 ppm (m, 10H, Ar-H); ¹³C NMR (75 MHz, CDCl₃):

δ_C = 21.2, 28.3, 28.7, 30.1 (d, ¹*J*_{C-P} = 138.6 Hz), 30.6 (d, ²*J*_{C-P} = 4.1 Hz), 31.1, 34.5 (d, ³*J*_{C-P} = 10.1 Hz), 35.6, 40.5 (d, ³*J*_{C-P} = 9.3 Hz), 66.9 (d, ²*J*_{C-P} = 6.6 Hz), 67.0 (d, ²*J*_{C-P} = 6.6 Hz), 80.2, 127.9, 127.9, 128.2, 128.3, 128.5, 128.9, 135.0, 136.4 (d, ³*J*_{C-P} = 6.2 Hz), 136.4 (d, ³*J*_{C-P} = 6.0 Hz), 139.1, 171.6 ppm; ³¹P NMR (121.5 MHz, CDCl₃): δ_P = 33.29 ppm; HRMS (ESI): calcd for C₃₂H₄₂O₅P [*M* + *H*]⁺: 537.2764, found: 537.2778.

tert-Butyl 3-((bis(benzyloxy)phosphoryl)methyl)-6-(*m*-tolyl)hexanoate (12 b): Prepared according to general procedure IV. Purification 2:1 hexane/EtOAc *v/v*; yield 45%; colorless oil. ¹H NMR (300 MHz, CDCl₃): δ_H = 1.39 (brs, 9H, tBu), 1.42–1.63 (m, 4H, -CH₂-), 1.78–1.98 (m, 2H, -CH₂-), 2.17–2.34 (m, 5H, Ph-CH₃, -CH₂-), 2.35–2.54 (m, 3H, -CH₂-, -CH₂-), 4.88–5.08 (m, 4H, -CH₂-Ph), 6.88–7.00 (m, 3H, Ar-H), 7.14 (t, *J* = 7.7 Hz, 1H, Ar-H), 7.28–7.37 ppm (m, 10H, Ar-H); ¹³C NMR (75 MHz, CDCl₃): δ_C = 21.6, 28.3, 28.6, 30.1 (d, ¹*J*_{C-P} = 138.6 Hz), 30.6 (d, ²*J*_{C-P} = 3.9 Hz), 34.6 (d, ³*J*_{C-P} = 10.3 Hz), 36.1, 40.5 (d, ³*J*_{C-P} = 10.3 Hz), 67.3 (d, ²*J*_{C-P} = 6.2 Hz), 80.6, 125.6, 126.7, 128.2, 128.4, 128.6, 128.8, 128.4, 136.7 (d, ³*J*_{C-P} = 7.1 Hz), 138.0, 142.5, 171.9 ppm; ³¹P NMR (121.5 MHz, CDCl₃): δ_P = 33.29 ppm; HRMS (ESI): calcd for C₃₂H₄₂O₅P [*M* + *H*]⁺: 537.2764, found: 537.2786.

tert-Butyl 3-((bis(benzyloxy)phosphoryl)methyl)-6-(4-methoxyphenyl)hexanoate (12 c): Prepared according to general procedure IV. Purification 2:1 hexane/EtOAc *v/v*; yield 53%; off-white oil. ¹H NMR (300 MHz, CDCl₃): δ_H = 1.39 (brs, 9H, tBu), 1.43–1.97 (m, 6H, -CH₂-), 2.17–2.52 (m, 5H, -CH₂-, -CH-), 3.77 (s, 3H, PhOCH₃), 4.88–5.10 (m, 4H, -CH₂-Ph), 6.79 (d, *J* = 9.1 Hz, 2H, Ar-H), 7.02 (d, *J* = 9.1 Hz, 2H, Ar-H), 7.26–7.44 ppm (m, 10H, Ar-H); ¹³C NMR (75 MHz, CDCl₃): δ_C = 28.0, 28.5, 29.8 (d, ¹*J*_{C-P} = 138.5 Hz), 30.3 (d, ²*J*_{C-P} = 3.9 Hz), 34.2 (d, ³*J*_{C-P} = 10.7 Hz), 34.9, 40.2 (d, ³*J*_{C-P} = 9.9 Hz), 55.2, 67.0 (d, ²*J*_{C-P} = 6.1 Hz), 67.0 (d, ²*J*_{C-P} = 6.7 Hz), 80.3, 113.7, 127.9, 128.3, 128.5, 129.2, 134.3, 136.4 (d, ³*J*_{C-P} = 5.3 Hz), 136.4 (d, ³*J*_{C-P} = 5.9 Hz), 157.7, 171.6 ppm; ³¹P NMR (121.5 MHz, CDCl₃): δ_P = 32.18 ppm; HRMS (ESI): calcd for C₃₂H₄₂O₆P [*M* + *H*]⁺: 553.2714, found: 553.2717.

tert-Butyl 3-((bis(benzyloxy)phosphoryl)methyl)-6-(3-methoxyphenyl)hexanoate (12 d): Prepared according to general procedure IV. Purification 2:1 hexane/EtOAc *v/v*; yield 47%; off-white oil. ¹H NMR (300 MHz, CDCl₃): δ_H = 1.39 (brs, 9H, tBu), 1.42–1.63 (m, 4H, -CH₂-), 1.76–1.93 (m, 2H, -CH₂-), 2.19–2.54 (m, 5H, -CH₂-, -CH-), 3.76 (s, 3H, PhOCH₃), 4.87–5.08 (m, 4H, -CH₂-Ph), 6.65–6.74 (m, 3H, Ar-H), 7.16 (t, *J* = 8.1 Hz, 1H, Ar-H), 7.28–7.36 ppm (m, 10H, Ar-H); ¹³C NMR (75 MHz, CDCl₃): δ_C = 28.3, 28.5, 30.2 (d, ¹*J*_{C-P} = 139.8 Hz), 30.6 (d, ²*J*_{C-P} = 4.1 Hz), 34.5 (d, ³*J*_{C-P} = 11.0 Hz), 36.1, 40.4 (d, ³*J*_{C-P} = 9.4 Hz), 55.3, 67.2 (d, ²*J*_{C-P} = 4.1 Hz), 67.3 (d, ²*J*_{C-P} = 4.3 Hz), 80.6, 111.2, 114.4, 121.0, 128.2, 128.6, 128.8, 129.5, 136.6 (d, ³*J*_{C-P} = 1.5 Hz), 136.7 (d, ³*J*_{C-P} = 6.0 Hz), 136.7 (d, ³*J*_{C-P} = 6.0 Hz), 144.1, 159.8, 171.9 ppm; ³¹P NMR (121.5 MHz, CDCl₃): δ_P = 33.24 ppm; HRMS (ESI): calcd for C₃₂H₄₂O₆P [*M* + *H*]⁺: 553.2714, found: 553.2717.

tert-Butyl 3-((bis(benzyloxy)phosphoryl)methyl)-6-(4-fluorophenyl)hexanoate (12 e): Prepared according to general procedure IV. Purification 2:1 hexane/EtOAc *v/v*; yield 43%; gold colored oil. ¹H NMR (300 MHz, CDCl₃): δ_H = 1.38 (brs, 9H, tBu), 1.42–1.61 (m, 4H, -CH₂-), 1.76–1.96 (m, 2H, -CH₂-), 2.16–2.34 (m, 2H, -CH₂-), 2.18–2.52 (m, 3H, -CH₂-, -CH-), 4.89–5.08 (m, 4H, -CH₂-Ph), 6.78–6.96 (m, 2H, Ar-H), 7.03 (m, 2H, Ar-H), 7.28–7.37 ppm (m, 10H, Ar-H); ¹³C NMR (75 MHz, CDCl₃): δ_C = 28.0, 28.4, 29.9 (d, ¹*J*_{C-P} = 138.9 Hz), 30.3 (d, ²*J*_{C-P} = 3.9 Hz), 34.1 (d, ³*J*_{C-P} = 10.2 Hz), 34.9, 40.2 (d, ³*J*_{C-P} = 10.2 Hz), 67.0 (m), 80.3, 114.9 (d, ²*J*_{C-F} = 20.4 Hz), 127.9, 128.3, 128.5, 129.6 (d, ³*J*_{C-F} = 7.7 Hz), 136.4 (d, ³*J*_{C-P} = 6.3 Hz), 137.8 (d, ⁴*J*_{C-F} = 3.3 Hz), 161.1 (d, ¹*J*_{C-F} = 243.0 Hz), 171.6 ppm; ³¹P NMR (121.5 MHz,

CDCl₃): $\delta_p = 33.00$ ppm; HRMS (ESI): calcd for C₃₁H₃₉FO₅P [M + H]⁺: 541.2514, found: 541.2519.

tert-Butyl 3-((bis(benzyloxy)phosphoryl)methyl)-6-(3-fluorophenyl)hexanoate (12 f): Prepared according to general procedure IV. Purification 2:1 hexane/EtOAc v/v; yield 47%; gold colored oil. ¹H NMR (300 MHz, CDCl₃): $\delta_H = 1.33$ – 1.40 (brs, 9H, tBu), 1.41–1.61 (m, 4H, -CH₂-), 1.72–1.97 (m, 2H, -CH₂-), 2.18–2.33 (2H, m, -CH₂-), 2.36–2.55 (m, 3H, -CH₂-, -CH-), 4.89–5.08 (m, 4H, CH₂-Ph), 6.76–6.90 (m, 3H, Ar-H), 7.19 (td, 1H, J = 6.08 Hz, 13.96 Hz, Ar-H), 7.29–7.39 ppm (m, 10H, Ar-H); ¹³C NMR (75 MHz, CDCl₃): $\delta_C = 28.2$, 28.3, 30.2 (d, ¹J_{C-P} = 139.9 Hz), 30.5 (d, ²J_{C-P} = 4.9 Hz), 34.4 (d, ³J_{C-P} = 10.8 Hz), 35.7, 40.5 (d, ³J_{C-P} = 9.8 Hz), 66.9 (d, ²J_{C-P} = 6.6 Hz), 67.0 (d, ²J_{C-P} = 6.4 Hz), 80.6, 112.8 (d, ²J_{C-F} = 21.0 Hz), 115.4 (d, ²J_{C-F} = 20.7 Hz), 124.2 (d, ⁴J_{C-F} = 3.1 Hz), 128.2, 128.6, 128.8, 129.9 (d, ³J_{C-F} = 8.3 Hz), 136.3 (d, ³J_{C-P} = 6.3 Hz), 136.4 (d, ³J_{C-P} = 6.4 Hz), 145.1 (d, ³J_{C-F} = 7.3 Hz), 162.8 (d, ¹J_{C-F} = 246.5 Hz), 171.8 ppm; ³¹P NMR (121.5 MHz, CDCl₃): $\delta_p = 33.16$ ppm; HRMS (ESI): calcd for C₃₁H₃₉FO₅P [M + H]⁺: 541.2514, found: 541.2515.

tert-Butyl 3-((bis(benzyloxy)phosphoryl)methyl)-6-(4-(trifluoromethyl)phenyl)hexanoate (12 g): Prepared according to general procedure IV. Purification 2:1 hexane/EtOAc v/v; yield 62% colorless oil. ¹H NMR (300 MHz, CDCl₃): $\delta_H = 1.37$ (brs, 9H, tBu), 1.41–1.64 (m, 4H, -CH₂-), 1.72–1.96 (m, 2H, -CH₂-), 2.18–2.61 (m, 5H, -CH₂-, -CH-), 4.90–5.09 (m, 4H, -CH₂-Ph), 7.19 (d, J = 8.0 Hz, 2H, Ar-H), 7.28–7.36 (m, 10H, Ar-H), 7.49 ppm (d, J = 8.0 Hz, 2H, Ar-H); ¹³C NMR (75 MHz, CDCl₃): $\delta_C = 28.3$, 28.4, 30.2 (d, ¹J_{C-P} = 138.2 Hz), 30.6 (d, ²J_{C-P} = 5.4 Hz), 34.4 (d, ³J_{C-P} = 10.8 Hz), 35.9, 40.6 (d, ³J_{C-P} = 9.2 Hz), 67.4 (d, ²J_{C-P} = 6.7 Hz), 67.5 (d, ²J_{C-P} = 6.6 Hz), 80.8, 124.6 (q, ¹J_{C-F} = 271.5 Hz), 125.5 (q, ³J_{C-F} = 3.8 Hz), 128.3, 128.5 (q, ²J_{C-F} = 27.1 Hz), 128.7, 128.9, 129.0, 136.7 (d, ³J_{C-P} = 6.0 Hz), 146.7, 171.9 ppm; ³¹P NMR (121.5 MHz, CDCl₃): $\delta_p = 31.86$ ppm; HRMS (ESI): calcd for C₃₂H₃₉F₃O₅P [M + H]⁺: 591.2482, found: 591.2487.

tert-Butyl 3-((bis(benzyloxy)phosphoryl)methyl)-6-(naphthalen-1-yl)hexanoate (12 h): Prepared according to general procedure IV. Purification 2:1 hexane/EtOAc v/v; yield 55%; colorless oil. ¹H NMR (300 MHz, CDCl₃): $\delta_H = 1.37$ (brs, 9H, tBu), 1.45–1.75 (m, 4H, -CH₂-), 1.77–1.94 (m, 2H, -CH₂-), 2.20–2.49 (m, 3H, -CH₂-, -CH-), 2.98 (t, J = 7.1 Hz, 2H, -CH₂-), 4.86–5.09 (m, 4H, -CH₂-Ph), 7.21–7.39 (m, 12H, Ar-H), 7.41–7.51 (m, 2H, Ar-H), 7.68 (d, J = 8.4 Hz, 1H, Ar-H), 7.80–7.86 (m, 1H, Ar-H), 7.93–7.99 ppm (m, 1H, Ar-H); ¹³C NMR (75 MHz, CDCl₃): $\delta_C = 27.8$, 28.2, 30.1 (d, ¹J_{C-P} = 138.8 Hz), 30.5 (d, ²J_{C-P} = 4.5 Hz), 33.1, 34.8 (d, ³J_{C-P} = 10.9 Hz), 40.3 (d, ³J_{C-P} = 10.0 Hz), 66.9 (d, ²J_{C-P} = 6.7 Hz), 7.2 (d, ²J_{C-P} = 6.4 Hz), 80.5, 123.9, 125.5, 125.6, 125.84, 126.0, 126.7, 128.1, 128.5, 128.7, 128.9, 131.9, 134.0, 135.3 (d, ³J_{C-P} = 6.4 Hz), 135.7 (d, ³J_{C-P} = 6.1 Hz), 138.5, 171.7 ppm; ³¹P NMR (121.5 MHz, CDCl₃): $\delta_p = 33.23$ ppm; HRMS (ESI): calcd for C₃₅H₄₂O₅P [M + H]⁺: 573.2764, found: 573.2761.

tert-Butyl 3-((bis(benzyloxy)phosphoryl)methyl)-6-(naphthalen-2-yl)hexanoate (12 i): Prepared according to general procedure IV. Purification 2:1 hexane/EtOAc v/v; yield 49%; colorless oil. ¹H NMR (300 MHz, CDCl₃): $\delta_H = 1.39$ (brs, 9H, tBu), 1.44–1.96 (m, 6H, -CH₂-), 2.21–2.53 (m, 3H, -CH₂-, -CH-), 2.71 (t, J = 7.2 Hz, 2H, -CH₂-), 4.91–5.10 (m, 4H, -CH₂-Ph), 7.25–7.49 (m, 13H, Ar-H), 7.56 (s, 1H, Ar-H), 7.73–7.83 ppm (m, 3H, Ar-H); ¹³C NMR (75 MHz, CDCl₃): $\delta_C = 28.0$, 28.1, 29.9 (d, ¹J_{C-P} = 139.1 Hz), 30.3 (d, ²J_{C-P} = 4.5 Hz), 34.2 (d, ³J_{C-P} = 10.5 Hz), 35.9, 40.2 (d, ³J_{C-P} = 9.8 Hz), 66.9 (d, ²J_{C-P} = 5.8 Hz), 67.00 (d, ²J_{C-P} = 6.9 Hz), 80.3, 125.0, 125.8, 126.3, 127.2, 127.3, 127.5, 127.8, 127.9, 128.3, 128.5, 131.9, 133.5, 136.4 (d, ³J_{C-P} = 6.2 Hz), 139.7, 171.6 ppm; ³¹P NMR (121.5 MHz, CDCl₃): $\delta_p = 32.13$ ppm; HRMS (ESI): calcd for C₃₅H₄₂O₅P [M + H]⁺: 573.2764, found: 573.2772.

tert-Butyl 6-([1,1'-biphenyl]-4-yl)-3-((bis(benzyloxy)phosphoryl)methyl)hexanoate (12 j): Prepared according to general procedure IV. Purification 2:1 hexane/EtOAc v/v; yield 71%; colorless oil. ¹H NMR (300 MHz, CDCl₃): $\delta_H = 1.38$ (brs, 9H, tBu), 1.42–1.99 (m, 6H, -CH₂-), 2.20–2.63 (m, 5H, -CH₂-, -CH-), 4.88–5.09 (m, 4H, -CH₂-Ph), 7.17 (d, J = 8.2 Hz, 2H, Ar-H), 7.25–7.60 ppm (m, 17H, Ar-H); ¹³C NMR (75 MHz, CDCl₃): $\delta_C = 28.0$, 28.2, 29.9 (d, ¹J_{C-P} = 138.5 Hz), 30.3 (d, ²J_{C-P} = 3.9 Hz), 34.2 (d, ³J_{C-P} = 10.9 Hz), 35.4, 40.2 (d, ³J_{C-P} = 9.3 Hz), 67.0 (d, ²J_{C-P} = 6.6 Hz), 67.1 (d, ²J_{C-P} = 6.4 Hz), 80.3, 126.9, 127.0, 127.9, 128.0, 128.3, 128.5, 128.6, 128.7, 136.3 (d, ³J_{C-P} = 6.1 Hz), 136.4 (d, ³J_{C-P} = 6.1 Hz), 138.6, 141.0, 141.3, 171.6 ppm; ³¹P NMR (121.5 MHz, CDCl₃): $\delta_p = 31.83$ ppm; HRMS (ESI): calcd for C₃₇H₄₄O₅P [M + H]⁺: 599.2921, found: 599.2928.

Dibenzyl (2-(2-((benzyloxy)(methyl)amino)-2-oxoethyl)-5-(p-tolyl)pentyl)phosphonate (13 a): Prepared according to general procedure V. Purification 3:1 hexane/acetone v/v; yield 71%; colorless oil. ¹H NMR (300 MHz, CDCl₃): $\delta_H = 1.34$ – 1.58 (m, 4H, -CH₂-), 1.72–2.05 (m, 3H, -CH₂-, -CH-), 2.30 (s, 3H, Ph-CH₃), 2.37–2.65 (m, 4H, -CH₂-), 3.13 (s, 3H, N-CH₃), 4.72 (s, 2H, NOCH₂Ph), 4.86–5.06 (m, 4H, -POCH₂Ph), 6.98 (d, J = 8.1 Hz, 2H, Ar-H), 7.05 (d, J = 8.1 Hz, 2H, Ar-H), 7.28–7.36 ppm (m, 15H, Ar-H); ¹³C NMR (75 MHz, CDCl₃): $\delta_C = 19.2$, 21.0, 28.7, 29.6 (d, ¹J_{C-P} = 139.3 Hz), 29.6 (d, ²J_{C-P} = 5.1 Hz), 33.5, 34.6 (d, ³J_{C-P} = 10.2 Hz), 35.4, 36.6 (d, ³J_{C-P} = 9.2 Hz), 67.1 (d, ²J_{C-P} = 6.3 Hz), 67.5 (d, ²J_{C-P} = 6.1 Hz), 76.1, 127.9, 127.9, 128.2, 128.3, 128.5, 128.6, 128.9, 128.9, 129.3, 134.5, 135.0, 136.5 (m), 139.3, 173.8 ppm; ³¹P NMR (121.5 MHz, CDCl₃): $\delta_p = 33.55$ ppm; HRMS (ESI): calcd for C₃₆H₄₃NO₅P [M + H]⁺: 600.2873, found: 600.2903.

Dibenzyl (2-(2-((benzyloxy)(methyl)amino)-2-oxoethyl)-5-(m-tolyl)pentyl)phosphonate (13 b): Prepared according to general procedure V. Purification 98:2 dichloromethane/MeOH v/v; yield 72%; colorless oil. ¹H NMR (300 MHz, CDCl₃): $\delta_H = 1.37$ – 1.59 (m, 4H, -CH₂-), 1.74–2.04 (m, 2H, -CH₂-), 2.30 (s, 3H, Ph-CH₃), 2.37–2.65 (m, 5H, -CH₂-, -CH-), 3.12 (s, 3H, N-CH₃), 4.72 (s, 2H, NOCH₂Ph), 4.89–5.05 (m, 4H, -POCH₂Ph), 6.86–7.00 (m, 3H, Ar-H), 7.13 (t, J = 7.4 Hz, 1H, Ar-H), 7.27–7.36 ppm (m, 15H, Ar-H); ¹³C NMR (75 MHz, CDCl₃): $\delta_C = 21.3$, 28.5, 28.6, 28.6 (d, ³J_{C-P} = 8.8 Hz), 29.5 (d, ¹J_{C-P} = 138.8 Hz), 29.6 (d, ²J_{C-P} = 4.9 Hz), 34.6 (d, ³J_{C-P} = 10.8 Hz), 35.7, 66.9 (m), 76.0, 125.3, 126.3, 127.8, 128.1, 128.2, 128.5, 128.6, 128.8, 129.1, 129.2, 136.4 (m), 137.6, 142.3, 171.9 ppm; ³¹P NMR (121.5 MHz, CDCl₃): $\delta_p = 33.54$ ppm; HRMS (ESI): calcd for C₃₆H₄₃NO₅P [M + H]⁺: 600.2873, found: 600.2883.

Dibenzyl (2-(2-((benzyloxy)(methyl)amino)-2-oxoethyl)-5-(4-methoxyphenyl)pentyl)phosphonate (13 c): Prepared according to general procedure V. Purification 3:1 hexane/acetone v/v; yield 57%; colorless oil. ¹H NMR (300 MHz, CDCl₃): $\delta_H = 1.34$ – 1.59 (m, 4H, -CH₂-), 1.73–2.04 (m, 2H, -CH₂-), 2.26–2.65 (m, 5H, -CH₂-, -CH-), 3.13 (s, 3H, N-CH₃), 3.75 (s, 3H, PhOCH₃), 4.72 (s, 2H, -NOCH₂Ph), 4.88–5.07 (m, 4H, -POCH₂Ph), 6.78 (d, J = 9.6 Hz, 2H, Ar-H), 7.00 (d, J = 9.6 Hz, 2H, Ar-H), 7.27–7.39 ppm (m, 15H, Ar-H); ¹³C NMR (75 MHz, CDCl₃): $\delta_C = 29.1$, 29.9 (d, ²J_{C-P} = 4.3 Hz), 30.0, 30.1 (d, ¹J_{C-P} = 136.9 Hz), 34.8 (d, ³J_{C-P} = 9.8 Hz), 35.1, 36.9 (d, ³J_{C-P} = 9.2 Hz), 55.5, 67.2 (d, ²J_{C-P} = 6.7 Hz), 67.3 (d, ²J_{C-P} = 6.1 Hz), 76.3, 113.9, 128.2, 128.5, 128.8, 128.9, 129.1, 129.5, 129.6, 134.7, 134.8 (d, ³J_{C-P} = 5.5 Hz), 136.7, 157.9, 173.5 ppm; ³¹P NMR (121.5 MHz, CDCl₃): $\delta_p = 32.35$ ppm; HRMS (ESI): calcd for C₃₆H₄₃NO₆P [M + H]⁺: 616.2823, found: 616.2830.

Dibenzyl (2-(2-((benzyloxy)(methyl)amino)-2-oxoethyl)-5-(3-methoxyphenyl)pentyl)phosphonate (13 d): Prepared according to general procedure V. Purification 5:1 dichloromethane/EtOAc v/v; yield 51%; colorless oil. ¹H NMR (300 MHz, CDCl₃): $\delta_H = 1.35$ – 1.61

(m, 4H, -CH₂-), 1.72–2.07 (m, 2H, -CH₂-), 2.27–2.67 (m, 5H, -CH₂-, -CH-), 3.12 (s, 3H, N-CH₃), 3.75 (s, 3H, PhOCH₃), 4.72 (s, 2H, -NOCH₂Ph), 4.87–5.07 (m, 4H, -POCH₂Ph), 6.64–6.74 (m, 3H, Ar-H), 7.16 (t, *J* = 7.9 Hz, 1H, Ar-H), 7.26–7.37 ppm (m, 15H, Ar-H); ¹³C NMR (75 MHz, CDCl₃): δ_c = 28.4, 29.5 (d, ²J_{C-P} = 4.5 Hz), 29.6 (d, ¹J_{C-P} = 138.4 Hz), 29.7, 34.5 (d, ³J_{C-P} = 10.3 Hz), 35.8, 36.6 (d, ³J_{C-P} = 9.0 Hz), 55.0, 66.8 (d, ²J_{C-P} = 6.7 Hz), 66.9 (d, ²J_{C-P} = 6.6 Hz), 76.0, 110.9, 114.0, 120.7, 127.8, 128.2, 128.4, 128.6, 128.8, 129.1, 129.2, 134.5, 136.4 (d, ³J_{C-P} = 6.1 Hz), 136.4 (d, ³J_{C-P} = 6.1 Hz), 144.0, 159.5, 173.7 ppm; ³¹P NMR (121.5 MHz, CDCl₃): δ_p = 32.31 ppm; HRMS (ESI): calcd for C₃₆H₄₃NO₆P [M + H]⁺: 616.2823, found: 616.2831.

Dibenzyl (2-(2-((benzyloxy)(methyl)amino)-2-oxoethyl)-5-(4-fluorophenyl)pentyl)phosphonate (13 e): Prepared according to general procedure V. Purification 3:1 hexane/acetone *v/v*; yield 71%; colorless oil. ¹H NMR (300 MHz, CDCl₃): δ_H = 1.36–1.56 (m, 4H, -CH₂-), 1.71–2.02 (m, 2H, -CH₂-), 2.23–2.50 (m, 5H, -CH₂-, -CH-), 3.13 (s, 3H, N-CH₃), 4.73 (s, 2H, -NOCH₂Ph), 4.87–5.09 (m, 4H, -POCH₂Ph), 6.85–7.06 (m, 4H, Ar-H), 7.27–7.39 ppm (m, 15H, Ar-H); ¹³C NMR (75 MHz, CDCl₃): δ_c = 28.6, 29.6 (d, ²J_{C-P} = 4.3 Hz), 29.7 (d, ³J_{C-P} = 10.0 Hz), 34.4 (d, ³J_{C-P} = 10.0 Hz), 34.9, 36.7 (d, ³J_{C-P} = 10.0 Hz), 37.0, 66.9 (d, ²J_{C-P} = 6.6 Hz), 67.0 (d, ²J_{C-P} = 6.3 Hz), 76.1, 114.9 (d, ²J_{C-F} = 21.8 Hz), 127.8 (d, ³J_{C-F} = 9.8 Hz), 127.9, 128.3, 128.6, 128.9, 129.2, 129.5, 134.5, 136.4 (d, ³J_{C-P} = 6.7 Hz), 137.9 (d, ⁴J_{C-F} = 4.2 Hz), 161.2 (d, ¹J_{C-F} = 242.42 Hz), 173.4 ppm; ³¹P NMR (121.5 MHz, CDCl₃): δ_p = 32.11 ppm; HRMS (ESI): calcd for C₃₅H₄₀FNO₅P [M + H]⁺: 604.2623, found: 604.2657.

Dibenzyl (2-(2-((benzyloxy)(methyl)amino)-2-oxoethyl)-5-(3-fluorophenyl)pentyl)phosphonate (13 f): Prepared according to general procedure V. Purification 3:1 hexane/acetone *v/v*; yield 69%; colorless oil. ¹H NMR (300 MHz, CDCl₃): δ_H = 1.32–1.58 (m, 4H, -CH₂-), 1.69–2.03 (m, 2H, -CH₂-), 2.25–2.53 (m, 5H, -CH₂-, -CH-), 3.13 (s, 3H, N-CH₃), 4.73 (s, 2H, -NOCH₂Ph), 4.86–5.09 (m, 4H, -POCH₂Ph), 6.73–7.92 (m, 3H, Ar-H), 7.14–7.38 ppm (m, 16H, Ar-H); ¹³C NMR (75 MHz, CDCl₃): δ_c = 28.2, 29.6 (d, ²J_{C-P} = 4.1 Hz), 29.7 (d, ¹J_{C-P} = 137.6 Hz), 31.6, 34.4 (d, ³J_{C-P} = 9.83 Hz), 35.5, 36.7 (d, ³J_{C-P} = 9.1 Hz), 66.9 (d, ²J_{C-P} = 6.7 Hz), 67.0 (d, ²J_{C-P} = 6.0 Hz), 76.1, 112.5 (d, ²J_{C-F} = 22.0 Hz), 115.1 (d, ²J_{C-F} = 22.0 Hz), 124.0 (d, ⁴J_{C-F} = 3.1 Hz), 127.9, 128.3, 128.5, 128.6, 128.9, 129.3, 129.5 (d, ³J_{C-F} = 8.6 Hz), 134.5, 136.4 (d, ³J_{C-P} = 6.1 Hz), 144.9 (d, ³J_{C-F} = 7.7 Hz), 162.8 (d, ¹J_{C-F} = 244.7 Hz), 173.25 ppm; ³¹P NMR (121.5 MHz, CDCl₃): δ_p = 33.43 ppm; HRMS (ESI): calcd for C₃₅H₄₀FNO₅P [M + H]⁺: 604.2623, found: 604.2656.

Dibenzyl (2-(2-((benzyloxy)(methyl)amino)-2-oxoethyl)-5-(4-(trifluoromethyl)phenyl)pentyl)phosphonate (13 g): Prepared according to general procedure V. Purification 3:1 hexane/acetone *v/v*; yield 55%; colorless oil. ¹H NMR (300 MHz, CDCl₃): δ_H = 1.34–1.59 (m, 4H, -CH₂-), 1.70–2.05 (m, 2H, -CH₂-), 2.25–2.64 (m, 5H, -CH₂-, -CH-), 3.12 (s, 3H, N-CH₃), 4.72 (s, 2H, -NOCH₂Ph), 4.87–5.08 (m, 4H, -POCH₂Ph), 7.17 (d, *J* = 8.2 Hz, 2H, Ar-H), 7.32 (m, 15H, Ar-H), 7.48 ppm (d, *J* = 8.2 Hz, 2H, Ar-H); ¹³C NMR (75 MHz, CDCl₃): δ_c = 28.2, 29.5 (d, ²J_{C-P} = 3.6 Hz), 29.7 (d, ¹J_{C-P} = 138.2 Hz), 32.8, 34.4 (d, ³J_{C-P} = 10.1 Hz), 35.5, 36.7 (d, ³J_{C-P} = 9.5 Hz), 66.9 (d, ²J_{C-P} = 6.4 Hz), 67.0 (d, ²J_{C-P} = 6.6 Hz), 76.1, 124.5 (q, ¹J_{C-F} = 272.7 Hz), 125.1 (q, ⁴J_{C-F} = 3.8 Hz), 127.9, 128.2 (q, ²J_{C-F} = 22.1 Hz), 128.3, 128.5, 128.6, 128.9, 129.2, 134.5, 136.4 (d, ³J_{C-P} = 6.3 Hz), 146.4, 173.8 ppm; ³¹P NMR (121.5 MHz, CDCl₃): δ_p = 33.43 ppm; HRMS (ESI): calcd for C₃₆H₄₀F₃NO₅P [M + H]⁺: 654.2591, found: 654.2601.

Dibenzyl (2-(2-((benzyloxy)(methyl)amino)-2-oxoethyl)-5-(naphthalen-1-yl)pentyl)phosphonate (13 h): Prepared according to general procedure V. Purification 98:2 dichloromethane/MeOH *v/v*; yield 44%; colorless oil. ¹H NMR (300 MHz, CDCl₃): δ_H = 1.50–2.04

(m, 6H, -CH₂-), 2.29–2.64 (m, 3H, -CH₂-, -CH-), 2.90–3.00 (m, 2H, -CH₂-), 3.12 (s, 3H, N-CH₃), 4.68 (s, 2H, -NOCH₂Ph), 4.88–5.05 (m, 4H, -POCH₂Ph), 7.19–7.40 (m, 17H, Ar-H), 7.43–7.50 (m, 2H, Ar-H), 7.66–7.72 (m, 1H, Ar-H), 7.80–7.86 (m, 1H, Ar-H), 7.93–7.99 ppm (m, 1H, Ar-H); ¹³C NMR (75 MHz, CDCl₃): δ_c = 28.1, 29.9 (d, ¹J_{C-P} = 138.4 Hz), 29.9 (d, ²J_{C-P} = 4.9 Hz), 33.2, 35.2 (d, ³J_{C-P} = 9.8 Hz), 36.9 (d, ³J_{C-P} = 8.5 Hz), 67.2 (d, ²J_{C-P} = 6.7 Hz), 67.3 (d, ²J_{C-P} = 6.7 Hz), 76.3, 124.1, 125.6, 125.8, 125.9, 126.1, 126.7, 128.2, 128.5, 128.8, 128.9, 129.0, 129.1, 129.5, 132.0, 134.1, 134.8, 136.7 (d, ³J_{C-P} = 6.4 Hz), 136.7 (d, ¹J_{C-P} = 6.1 Hz), 138.8, 168.0 ppm; ³¹P NMR (121.5 MHz, CDCl₃): δ_p = 33.49 ppm; HRMS (ESI): calcd for C₃₉H₄₃NO₅P [M + H]⁺: 636.2873, found: 636.2880.

Dibenzyl (2-(2-((benzyloxy)(methyl)amino)-2-oxoethyl)-5-(naphthalen-2-yl)pentyl)phosphonate (13 i): Prepared according to general procedure V. Purification 3:1 hexane/acetone *v/v*; yield 78%; colorless oil. ¹H NMR (300 MHz, CDCl₃): δ_H = 1.37–2.02 (m, 6H, -CH₂-), 2.26–2.75 (m, 5H, -CH₂-, -CH-), 3.11 (s, 1H, N-CH₃), 4.71 (s, 2H, -NOCH₂Ph), 4.85–5.08 (m, 4H, -POCH₂Ph), 7.21–7.34 (m, 16H, Ar-H), 7.36–7.47 (m, 2H, Ar-H), 7.53 (s, 1H, Ar-H), 7.70–7.81 ppm (m, 3H, Ar-H); ¹³C NMR (75 MHz, CDCl₃): δ_c = 28.7, 29.9 (d, ²J_{C-P} = 3.9 Hz), 30.0 (d, ¹J_{C-P} = 138.8 Hz), 32.9, 34.8 (d, ³J_{C-P} = 10.4 Hz), 36.2, 36.9 (d, ³J_{C-P} = 9.1 Hz), 67.2 (d, ²J_{C-P} = 6.6 Hz), 67.3 (d, ²J_{C-P} = 6.0 Hz), 76.3, 125.3, 126.0, 126.6, 127.5, 127.6, 127.8, 128.0, 128.2, 128.5, 128.8, 128.9, 129.1, 129.5, 132.2, 133.8, 134.8, 136.7 (d, ²J_{C-P} = 6.6 Hz), 136.8 (d, ²J_{C-P} = 6.2 Hz), 140.1, 170.4 ppm; ³¹P NMR (121.5 MHz, CDCl₃): δ_p = 33.49 ppm; HRMS (ESI): calcd for C₃₉H₄₃NO₅P [M + H]⁺: 636.2873, found: 636.2880.

Dibenzyl (5-([1,1'-biphenyl]-4-yl)-2-(2-((benzyloxy)(methyl)amino)-2-oxoethyl)pentyl)phosphonate (13 j): Prepared according to general procedure V. Purification 97:3 dichloromethane/EtOAc *v/v*; yield 68%; colorless oil. ¹H NMR (300 MHz, CDCl₃): δ_H = 1.38–1.64 (m, 4H, -CH₂-), 1.75–2.04 (m, 2H, -CH₂-), 2.28–2.66 (m, 5H, -CH₂-, -CH-), 3.13 (s, 3H, N-CH₃), 4.72 (s, 2H, -NOCH₂Ph), 4.89–5.07 (m, 4H, -POCH₂Ph), 7.11–7.19 (m, 3H, Ar-H), 7.25–7.60 ppm (m, 21H, Ar-H); ¹³C NMR (75 MHz, CDCl₃): δ_c = 28.5, 29.6 (d, ²J_{C-P} = 4.7 Hz), 30.3, 29.6 (d, ¹J_{C-P} = 138.2 Hz), 34.5 (d, ³J_{C-P} = 10.2 Hz), 35.4, 36.6 (d, ³J_{C-P} = 10.2 Hz), 66.9 (d, ²J_{C-P} = 6.1 Hz), 70.0 (d, ²J_{C-P} = 6.6 Hz), 76.0, 126.9, 127.9, 128.2, 128.5, 128.6, 128.7, 128.8, 128.9, 129.2, 134.5, 136.4 (d, ³J_{C-P} = 6.4 Hz), 138.5, 141.0, 141.5, 172.6 ppm; ³¹P NMR (121.5 MHz, CDCl₃): δ_p = 32.33 ppm; HRMS (ESI): calcd for C₄₁H₄₅NO₅P [M + H]⁺: 662.3030, found: 662.3039.

Sodium hydrogen (2-(2-(hydroxy(methyl)amino)-2-oxoethyl)-5-(*p*-tolyl)pentyl)phosphonate (6 a): White powder. Prepared from compound **13 a** (150 mg, 0.25 mmol) according to general procedure VI; quantitative yield. ¹H NMR (300 MHz, D₂O): δ_H = 1.29–1.78 (m, 6H, -CH₂-), 1.94–2.41 (m, 4H, -CH-, Ph-CH₃), 2.45–2.70 (m, 4H, -CH₂-), 3.01 (s, 5/6 of N-CH₃), 3.23 (s, 1/6 of N-CH₃), 6.89–7.23 ppm (m, 4H, Ar-H); ¹³C NMR (75 MHz, D₂O): δ_c = 20.0, 27.6, 30.5 (d, ²J_{C-P} = 4.3 Hz), 31.6 (d, ¹J_{C-P} = 130.7 Hz), 34.1 (d, ³J_{C-P} = 12.7 Hz), 34.5, 37.0, 39.2 (d, ¹J_{C-P} = 7.1 Hz), 128.4, 128.9, 135.4, 139.8, 177.8 ppm; ³¹P NMR (121.5 MHz, D₂O): δ_p = 25.97 ppm; HRMS (ESI): calcd for C₁₅H₂₃NO₅P [M - H]⁻: 328.1319, found: 328.1320.

Sodium hydrogen (2-(2-(hydroxy(methyl)amino)-2-oxoethyl)-5-(*m*-tolyl)pentyl)phosphonate (6 b): White powder. Prepared from compound **13 b** (150 mg, 0.25 mmol) according to general procedure VI; quantitative yield. ¹H NMR (300 MHz, D₂O): δ_H = 1.22–1.69 (m, 6H, -CH₂-), 1.99–2.23 (m, 1H, -CH-), 2.28 (s, 3H, Ph-CH₃), 2.49–2.68 (m, 4H, -CH₂-), 3.18 (s, 5/6 of N-CH₃), 3.35 (s, 1/6 of N-CH₃), 7.02–7.15 (m, 3H, Ar-H), 7.23 ppm (app t, *J* = 7.4 Hz, 1H, Ar-H); ¹³C NMR (75 MHz, D₂O): δ_c = 20.5, 28.4, 32.2 (d, ²J_{C-P} = 4.1 Hz), 33.4 (d, ¹J_{C-P} = 130.7 Hz), 35.3, 35.4 (d, ³J_{C-P} = 9.8 Hz), 36.2, 36.3 (d,

$^3J_{C-P}=5.9$ Hz), 125.8, 126.5, 128.7, 129.4, 138.7, 143.8, 174.4 ppm; ^{31}P NMR (121.5 MHz, D_2O): rotamers at $\delta_p=22.14$ and 22.25 ppm; HRMS (ESI): calcd for $C_{15}H_{23}NO_5P [M-H]^-$: 328.1319, found: 328.1318.

Sodium hydrogen (2-(2-(hydroxy(methyl)amino)-2-oxoethyl)-5-(4-methoxyphenyl)pentyl)phosphonate (6c): White powder. Prepared from compound **13c** (125 mg, 0.20 mmol) according to general procedure VI; quantitative yield. 1H NMR (300 MHz, D_2O): $\delta_H=1.23$ – 1.66 (m, 6H, $-CH_2-$), 2.01 – 2.26 (m, 1H, $-CH-$), 2.47 – 2.67 (m, 4H, $-CH_2-$), 3.17 (s, 5/6 of $N-CH_3$), 3.34 (s, 1/6 of $N-CH_3$), 3.78 (s, 3H, $PhOCH_3$), 6.91 (m, 2H, Ar-H), 7.21 ppm (m, 2H, Ar-H); ^{13}C NMR (75 MHz, D_2O): $\delta_C=28.3$, 32.0 (d, $^2J_{C-P}=4.0$ Hz), 33.3 (d, $^1J_{C-P}=129.9$ Hz), 34.4 , 35.1 (d, $^3J_{C-P}=10.7$ Hz), 36.1 , 36.4 (d, $^3J_{C-P}=6.2$ Hz), 55.6 , 114.1 , 129.9 , 136.2 , 156.9 , 175.0 ppm; ^{31}P NMR (121.5 MHz, D_2O): $\delta_p=22.48$ ppm; HRMS (ESI): calcd for $C_{15}H_{23}NO_6P [M-H]^-$: 344.1268, found: 344.1269.

Sodium hydrogen (2-(2-(hydroxy(methyl)amino)-2-oxoethyl)-5-(3-methoxyphenyl)pentyl)phosphonate (6d): White powder. Prepared from compound **13d** (150 mg, 0.24 mmol) according to general procedure VI; quantitative yield. 1H NMR (300 MHz, D_2O): $\delta_H=1.24$ – 1.69 (m, 6H, $-CH_2-$), 2.02 – 2.26 (m, 1H, $-CH-$), 2.51 – 2.66 (m, 4H, $-CH_2-$), 3.17 (s, 5/6 of $N-CH_3$), 3.34 (s, 1/6 of $N-CH_3$), 3.79 (s, 3H, $PhOCH_3$), 6.77 – 6.93 (m, 3H, Ar-H), 7.26 ppm (app t, $J=7.9$ Hz, 1H, Ar-H); ^{13}C NMR (75 MHz, D_2O): $\delta_C=28.0$, 31.8 (d, $^2J_{C-P}=4.1$ Hz), 33.1 (d, $^1J_{C-P}=130.2$ Hz), 35.1 (d, $^3J_{C-P}=10.6$ Hz), 35.4 , 36.1 , 36.5 (d, $^3J_{C-P}=7.3$ Hz), 55.4 , 111.5 , 114.2 , 121.7 , 129.8 , 145.5 , 159.0 , 175.2 ppm; ^{31}P NMR (121.5 MHz, D_2O): $\delta_p=21.72$ ppm; HRMS (ESI): calcd for $C_{15}H_{23}NO_6P [M-H]^-$: 344.1268, found: 344.1269.

Sodium hydrogen (5-(4-fluorophenyl)-2-(2-(hydroxy(methyl)amino)-2-oxoethyl)pentyl)phosphonate (6e): White powder. Prepared from compound **13e** (100 mg, 0.17 mmol) according to general procedure VI; quantitative yield. 1H NMR (300 MHz, D_2O): $\delta_H=1.14$ – 1.68 (m, 6H, $-CH_2-$), 1.92 – 2.20 (m, 1H, $-CH-$), 2.42 – 2.66 (m, 4H, $P-CH_2-$, CH_2-CON-), 3.14 (s, 5/6 of $N-CH_3$), 3.27 (s, 1/6 of $N-CH_3$), 6.97 – 7.09 (m, 2H, Ar-H), 7.20 – 7.33 ppm (m, 2H, Ar-H); ^{13}C NMR (75 MHz, D_2O): $\delta_C=28.0$, 31.4 (d, $^2J_{C-P}=4.5$ Hz), 33.9 (d, $^1J_{C-P}=139.3$ Hz), 34.6 (d, $^3J_{C-P}=8.1$ Hz), 34.7 , 36.3 (d, $^3J_{C-P}=8.3$ Hz), 37.1 , 114.7 (d, $^2J_{C-F}=21.2$ Hz), 129.9 (d, $^3J_{C-F}=8.3$ Hz), 139.2 (d, $^4J_{C-F}=3.7$ Hz), 160.7 (d, $^1J_{C-F}=239.1$ Hz), 169.0 ppm; ^{31}P NMR (121.5 MHz, D_2O): rotamers at $\delta_p=21.40$, 21.50 ppm; HRMS (ESI): calcd for $C_{14}H_{21}FNO_5P [M-H]^-$: 332.1069, found: 332.1088.

Sodium hydrogen (5-(3-fluorophenyl)-2-(2-(hydroxy(methyl)amino)-2-oxoethyl)pentyl)phosphonate (6f): White powder. Prepared from compound **13f** (130 mg, 0.22 mmol) according to general procedure VI; quantitative yield. 1H NMR (300 MHz, D_2O): $\delta_H=1.23$ – 1.68 (m, 6H, $-CH_2-$), 2.02 – 2.23 (m, 1H, $-CH-$), 2.50 – 2.69 (m, 4H, $-CH_2-$), 3.17 (s, 5/6 of $N-CH_3$), 3.35 (s, 1/6 of $N-CH_3$), 6.88 – 7.10 (m, 3H, Ar-H), 7.25 – 7.34 ppm (m, 1H, Ar-H); ^{13}C NMR (75 MHz, D_2O): $\delta_C=27.9$, 31.9 (d, $^2J_{C-P}=4.1$ Hz), 33.1 (d, $^1J_{C-P}=129.1$ Hz), 35.0 (d, $^3J_{C-P}=8.2$ Hz), 35.1 , 36.1 , 36.4 (d, $^3J_{C-P}=7.0$ Hz), 112.5 (d, $^2J_{C-F}=23.32$ Hz), 115.3 (d, $^2J_{C-F}=21.9$ Hz), 124.6 (d, $^4J_{C-F}=2.7$ Hz), 130.1 (d, $^3J_{C-F}=8.7$ Hz), 146.2 (d, $^3J_{C-F}=8.7$ Hz), 162.9 (d, $^1J_{C-F}=247.1$ Hz), 175.0 ppm; ^{31}P NMR (121.5 MHz, D_2O): $\delta_p=22.75$ ppm; HRMS (ESI): calcd for $C_{14}H_{20}FNO_5P [M-H]^-$: 332.1069, found: 332.1067.

Sodium hydrogen (2-(2-(hydroxy(methyl)amino)-2-oxoethyl)-5-(4-(trifluoromethyl)phenyl)pentyl)phosphonate (6g): White powder. Prepared from compound **13g** (150 mg, 0.25 mmol) according to general procedure VI; quantitative yield. 1H NMR (300 MHz, D_2O): $\delta_H=1.27$ – 1.71 (m, 6H, $-CH_2-$), 2.00 – 2.26 (m, 1H, $-CH-$), 2.50 – 2.61 (m, 2H, $-CH_2-$), 2.66 (t, $J=7.4$ Hz, 2H, $-CH_2-$), 3.16 (s, 5/6 of $N-CH_3$), 3.34 (s, 1/6 of $N-CH_3$), 3.79 – 7.40 (d, $J=7.9$ Hz, 2H, Ar-

H), 7.61 ppm (d, $J=7.9$ Hz, 2H, Ar-H); ^{13}C NMR (75 MHz, D_2O): $\delta_C=27.5$, 29.5 , 31.5 (d, $^2J_{C-P}=4.1$ Hz), 32.8 (d, $^1J_{C-P}=130.7$ Hz), 34.5 (d, $^3J_{C-P}=11.0$ Hz), 34.9 , 35.8 , 36.3 (d, $^3J_{C-P}=6.8$ Hz), 124.4 (q, $^1J_{C-F}=270.5$ Hz), 125.0 (q, $^3J_{C-F}=4.1$ Hz), 128.9 (app s), 147.6 , 174.9 ppm; ^{31}P NMR (121.5 MHz, D_2O): $\delta_p=21.49$ ppm; HRMS (ESI): calcd for $C_{15}H_{20}F_3NO_5P [M-H]^-$: 382.1037, found: 382.1039.

Sodium hydrogen (2-(2-(hydroxy(methyl)amino)-2-oxoethyl)-5-(naphthalen-1-yl)pentyl)phosphonate (6h): White powder. Prepared from compound **13h** (150 mg, 0.24 mmol) according to general procedure VI; quantitative yield. 1H NMR (300 MHz, D_2O): $\delta_H=1.38$ – 1.84 (m, 6H, $-CH_2-$), 2.02 – 2.27 (m, 1H, $-CH-$), 2.46 – 2.65 (m, 2H, $-CH_2-$), 3.07 (t, $J=7.6$ Hz, 2H, $-CH_2-$), 3.13 (s, 5/6 of $N-CH_3$), 3.24 (s, 1/6 of $N-CH_3$), 7.39 – 7.62 (m, 4H, Ar-H), 7.78 (dd, $J=2.4$ Hz, 7.4 Hz, 1H, Ar-H), 7.92 (dd, $J=2.4$ Hz, 8.1 Hz, 1H, Ar-H), 8.18 ppm (d, $J=8.1$ Hz, 1H, Ar-H); ^{13}C NMR (75 MHz, D_2O): $\delta_C=27.8$, 32.1 (d, $^2J_{C-P}=4.5$ Hz), 32.7 , 33.8 (d, $^1J_{C-P}=129.3$ Hz), 34.5 , 35.7 (d, $^3J_{C-P}=10.8$ Hz), 36.4 (d, $^3J_{C-P}=7.6$ Hz), 36.6 , 124.4 , 126.1 , 126.2 , 126.3 , 126.4 , 128.8 , 131.6 , 133.7 , 139.7 , 172.7 ppm; ^{31}P NMR (121.5 MHz, D_2O): rotamers at $\delta_p=21.94$, 22.18 ppm; HRMS (ESI): calcd for $C_{18}H_{23}NO_5P [M-H]^-$: 364.1319, found: 364.1315.

Sodium hydrogen (2-(2-(hydroxy(methyl)amino)-2-oxoethyl)-5-(naphthalen-2-yl)pentyl)phosphonate (6i): White powder. Prepared from compound **13i** (150 mg, 0.24 mmol) according to general procedure VI; quantitative yield. 1H NMR (300 MHz, D_2O): $\delta_H=1.23$ – 1.80 (m, 6H, $-CH_2-$), 2.01 – 2.29 (m, 1H, $-CH-$), 2.46 – 2.65 (m, 2H, $-CH_2-$), 2.78 (t, $J=7.8$ Hz, 2H, $-CH_2-$), 3.12 (s, 5/6 of $N-CH_3$), 3.30 (s, 1/6 of $N-CH_3$), 7.44 – 7.55 (m, 3H, Ar-H), 7.77 (s, 1H, Ar-H), 7.84 – 7.92 ppm (m, 3H, Ar-H); ^{13}C NMR (75 MHz, D_2O): $\delta_C=29.8$, 31.8 (d, $^2J_{C-P}=3.7$ Hz), 34.1 (d, $^1J_{C-P}=130.8$ Hz), 35.0 (d, $^3J_{C-P}=10.9$ Hz), 35.8 , 36.5 (d, $^3J_{C-P}=8.0$ Hz), 37.3 , 125.5 , 126.3 , 126.4 , 127.5 , 127.7 , 127.9 , 128.1 , 131.7 , 133.5 , 141.6 , 169.7 ppm; ^{31}P NMR (121.5 MHz, D_2O): $\delta_p=22.48$ ppm; HRMS (ESI): calcd for $C_{18}H_{23}NO_5P [M-H]^-$: 364.1319, found: 364.1315.

Sodium hydrogen (5-([1,1'-biphenyl]-4-yl)-2-(2-(hydroxy(methyl)amino)-2-oxoethyl)pentyl)phosphonate (6j): White powder. Prepared from compound **13j** (200 mg, 0.30 mmol) according to general procedure VI; quantitative yield. 1H NMR (300 MHz, D_2O): $\delta_H=1.23$ – 1.73 (m, 6H, $-CH_2-$), 1.98 – 2.24 (m, 1H, $-CH-$), 2.42 – 2.70 (m, 4H, $-CH_2-$), 3.14 (s, 5/6 of $N-CH_3$), 3.30 (s, 1/6 of $N-CH_3$), 7.35 – 7.53 (m, 5H, Ar-H), 7.58 – 7.71 ppm (m, 4H, Ar-H); ^{13}C NMR (75 MHz, D_2O): $\delta_C=27.9$, 31.5 (d, $^2J_{C-P}=4.1$ Hz), 33.0 (d, $^1J_{C-P}=130.1$ Hz), 34.5 (d, $^2J_{C-P}=10.1$ Hz), 35.0 , 36.3 (d, $^3J_{C-P}=8.38$ Hz), 37.1 , 126.7 , 126.8 , 127.4 , 129.0 , 129.3 , 137.8 , 140.4 , 143.1 , 169.2 ppm; ^{31}P NMR (121.5 MHz, D_2O): rotamers at $\delta_p=21.37$, 21.54 ppm; HRMS (ESI): calcd for $C_{20}H_{25}NO_5P [M-H]^-$: 390.1476, found: 390.1479.

X-ray crystallography: Protein was produced as described earlier.^[23] The water-soluble ligands (**6a**, **6b**, **6c**, **6d**, **6f**, **6g**, **6h**) were incubated (1 mM final concentration) with the protein solution (0.3 mM in 20 mM Tris-HCl, pH 7.8, 200–300 mM NaCl, 5% (v/v) glycerol, 2 mM dithiothreitol and 1 mM $MnCl_2$) for 10–15 min at 20 °C before the co-crystallization experiments were set up in 2-well MRC plates (Molecular Dimensions, UK) with a Mosquito robot (TTP Labtech, UK). Reservoir solutions consisted of 40 μ L, and the sitting droplets contained equal volumes (100 nL each) of the protein–ligand mixture and reservoir solution. Previous screening^[23] had shown the Morpheus screen^[34] was highly effective for this protein, and crystals (0.1 \times 0.1 \times 0.1 mm) appeared in 1–3 days at 20 °C under multiple conditions (Supporting Information Table S1). Crystals were harvested without further cryoprotection, and plunged into liquid nitrogen for transport to the relevant synchrotron beamline.

Diffraction data were collected at 100 K at the European Synchrotron Radiation Facility (ESRF, Grenoble, France) or at Diamond, Oxford, England (Supporting Information Table S2). All crystals had the symmetry of the triclinic space group P_1 , and could be classified into the same one of the two related groups of P_1 cells discussed earlier.^[23] Diffraction images were processed and scaled with XDS^[35] and SCALA^[36] respectively, using the CCP4 package.^[37] Rigid-body refinement was used for initial placement of the structures, to maintain a similar position relative to that observed earlier. Structures were then subjected to alternating rounds of reciprocal space refinement with REFMAC5^[38] and manual rebuilding with O.^[39] Solvent was added using the *water* tools in O. The ligands and respective stereochemical restraints were built and generated with the *qds* tools in O. Refinement restraints were then generated from the fitted models by REFMAC5, and manually edited as needed. Hydroxamate groups were restrained to planarity, and metal-coordination target distances were taken from Harding.^[40] Complete data collection and refinement statistics are included in Supporting Information Table S2.

Briefly, the structures of the seven new β -substituted enzyme-inhibitor complexes (**6a**, **6b**, **6c**, **6d**, **6f**, **6g**, **6h**) were solved at resolutions of 1.55, 1.8, 1.7, 1.7, 1.7, 1.6 and 1.4 Å, respectively, and refined to crystallographic *R*-factors of 18.6, 17.7, 18.2, 16.9, 18.2, 18.0 and 18.7% (*R*_{free} values are 20.5, 20.4, 21.1, 20.3, 20.8 and 20.7%, respectively). Each complex has a dimer in the asymmetric unit, with a manganese ion and ligand in each active site. Although the new compounds were synthesized as racemic mixtures, the high resolution of the study (e.g., Figure 4a) allowed us to define the respective enantiomer of each ligand. The overall electron density is of high quality, and complete models of the enzyme are deposited for residues 77–486 in each chain. Density for residues in the active-site flap is discussed in the main text, and described further in Supporting Information Table S3. Structural comparisons were made with the *lsq* commands in O with close-pair *C* α cutoffs (1.0 Å *C* α –*C* α separations).^[41] Figures were created in O, using secondary structure assignments from the *yasspa* algorithm, and rendered in Molray.^[42] Structures of the various complexes were deposited at the RCSB Protein Data Bank as follows: **6a** (5JMW), **6b** (5JOO), **6c** (5JBI), **6d** (5JC1), **6f** (5JMP), **6g** (5JNL) and **6h** (5JAZ). Electron density for each entry is available at the Uppsala Electron Density Server.^[43]

Supporting Information: Additional experimental details are presented, including comparisons of *pI*C₅₀ for EcDxr and PfDxr, comparisons of *pI*C₅₀ with crystallographic temperature factors and fit to electron density, crystallization conditions used in the reported X-ray structures, statistics for data collection and refinement, and summary of electron density in residues of the flap.

Abbreviations: Bn: benzyl, DOXP: 1-deoxy-D-xylulose 5-phosphate, DMAP: 4-(dimethylamino)pyridine, Dxr: 1-deoxy-D-xylulose-5-phosphate reductoisomerase, EcDxr: *Escherichia coli* Dxr, EDC: *N*-(3-dimethylaminopropyl)-*N'*-ethylcarbodiimide, MEP: 2-C-methyl-D-erythritol-3-phosphate, PfDxr: *Plasmodium falciparum* Dxr, RMS: root mean square, RT: room temperature, TFA: trifluoroacetic acid, THF: tetrahydrofuran.

Acknowledgements

We acknowledge funding from the European Community's Seventh Framework Programme (FP7/2007–2013) under BioStruct-X (grant agreement no. 283570). T.A.J. and S.L.M. were supported by the Swedish Research Council (VR), FORMAS, and Uppsala Uni-

versity. S.V.C. received support from FWO Flanders. R.C. received a doctoral scholarship from the Special Research Fund of the University of Gent. We thank An Matheussen for running the *in vitro* antiparasite evaluation, and Izet Karalic for technical assistance.

Keywords: antibiotics · antiprotozoal agents · oxidoreductases · structural biology · structure–activity relationships

- [1] World Malaria Report 2015, World Health Organization: <http://www.who.int/malaria/publications/world-malaria-report-2015/report/en/> (ISBN: 978 924 156 5158).
- [2] H. Jomaa, J. Wiesner, S. Sanderbrand, B. Altincicek, C. Weidemeyer, M. Hintz, I. Turbachova, M. Eberl, J. Zeidler, H. K. Lichtenthaler, D. Soldati, E. Beck, *Science* **1999**, *285*, 1573–1576.
- [3] B. M. Lange, T. Rujan, W. Martin, R. Croteau, *Proc. Natl. Acad. Sci. USA* **2000**, *97*, 13172–13177.
- [4] T. Kuzuyama, *Biosci. Biotechnol. Biochem.* **2002**, *66*, 1619–1627.
- [5] F. Rohdich, A. Bacher, W. Eisenreich, *Biochem. Soc. Trans.* **2005**, *33*, 785–791.
- [6] S. Takahashi, T. Kuzuyama, H. Watanabe, H. A. Seto, *Proc. Natl. Acad. Sci. USA* **1998**, *95*, 9879–9884.
- [7] M. Rohmer, *Nat. Prod. Rep.* **1999**, *16*, 565–574.
- [8] T. Kuzuyama, T. Shimizu, S. Takahashi, H. Seto, *Tetrahedron Lett.* **1998**, *39*, 7913–7916.
- [9] J. Zeidler, J. Schwender, C. Müller, J. Wiesner, C. Weidemeyer, E. Beck, H. Jomaa, H. K. Lichtenthaler, *Z. Naturforsch.* **1998**, *53c*, 980–986.
- [10] T. Murakawa, H. Sakamoto, S. Fukada, T. Konishi, M. Nishida, *Antimicrob. Agents Chemother.* **1982**, *21*, 224–230.
- [11] S. Borrmann, I. Lundgren, S. Oyakhrome, B. Impouma, P. B. Matsiegui, A. A. Adegnika, S. Issifou, J. F. J. Kun, D. Hutchinson, J. Wiesner, H. Jomaa, P. G. Kremsner, *Antimicrob. Agents Chemother.* **2006**, *50*, 2713–2718.
- [12] M. Lanaspá, C. Moraleda, S. Machevo, R. González, B. Serrano, E. Macete, P. Cisteró, A. Mayor, D. Hutchinson, P. G. Kremsner, P. Alonso, C. Menéndez, Q. Bassata, *Antimicrob. Agents Chemother.* **2012**, *56*, 2923–2928.
- [13] E. R. Jackson, C. S. Dowd, *Curr. Top. Med. Chem.* **2012**, *12*, 706–728.
- [14] I. Hale, P. M. O'Neill, N. G. Berry, A. Odom, R. Sharma, *MedChemComm* **2012**, *3*, 418–433.
- [15] T. Masini, A. K. H. Hirsch, *J. Med. Chem.* **2014**, *57*, 9740–9763.
- [16] L. M. Henriksson, T. Unge, J. Carlsson, J. Åqvist, S. L. Mowbray, T. A. Jones, *J. Biol. Chem.* **2007**, *282*, 19905–19916.
- [17] A. Mac Sweeney, R. Lange, R. P. M. Fernandes, H. Schulz, G. E. Dale, A. Douangamath, P. J. Proteau, C. Oefner, *J. Mol. Biol.* **2005**, *345*, 115–127.
- [18] T. Umeda, N. Tanaka, Y. Kusakabe, M. Nakanishi, Y. Kitade, K. T. Nakamura, *Sci. Rep.* **2011**, *1*, 9.
- [19] J. Xue, J. Diao, G. Cai, L. Deng, B. Zheng, Y. Yao, Y. Song, *ACS Med. Chem. Lett.* **2013**, *4*, 278–282.
- [20] T. Masini, B. S. Kroezen, A. K. Hirsch, *Drug Discovery Today* **2013**, *18*, 1256–1262.
- [21] S. A. Kholodar, G. Tomblin, J. Liu, Z. Tan, C. L. Allen, A. M. Gulick, A. S. Murkin, *Biochemistry* **2014**, *53*, 3423–3431.
- [22] L. Deng, K. Endo, M. Kato, G. Cheng, S. Yajima, Y. Song, *Med. Chem. Lett.* **2011**, *2*, 165–170.
- [23] R. Chofor, S. Sooriyaarachchi, M. D. P. Risseeuw, T. Bergfors, J. Pouyez, C. Johny, A. Haymond, A. Everaert, C. S. Dowd, L. Maes, T. Coenye, A. Alex, R. D. Couch, T. A. Jones, J. Wouters, S. L. Mowbray, S. Van Calenbergh, *J. Med. Chem.* **2015**, *58*, 2988–3001.
- [24] C. Björkelid, T. Bergfors, T. Unge, S. L. Mowbray, T. A. Jones, *Acta Crystallogr. Sect. D* **2012**, *68*, 134–143.
- [25] S. Jawaid, H. Seidle, W. Zhou, H. Abdirahman, M. Abadeer, J. H. Hix, M. L. van Hoek, R. D. Couch, *PLOS ONE* **2009**, *4*, e8288.
- [26] T. Verbrugghen, P. Cos, L. Maes, S. Van Calenbergh, *J. Med. Chem.* **2010**, *53*, 5342–5346.
- [27] T. Haemers, J. Wiesner, S. Van Poecke, J. Goeman, D. Henschker, E. Beck, H. Jomaa, S. Van Calenbergh, *Bioorg. Med. Chem. Lett.* **2006**, *16*, 1888–1891.

- [28] D. Giessmann, P. Heidler, T. Haemers, S. Van Calenberg, A. Reichenberg, J. Jomaa, C. Weidemeyer, S. Sanderbrand, J. Wiesner, A. Link, *Chem. Biodiversity* **2008**, *5*, 643–656.
- [29] P. Cos, A. J. Vlietinck, D. Van den Berghe, L. Maes, *J. Ethnopharmacol.* **2006**, *106*, 290–302.
- [30] R. J. Read, *Acta Crystallogr. Sect. A* **1986**, *42*, 140–149.
- [31] L. Deng, J. Diao, P. Chen, V. Pujari, Y. Yao, G. Cheng, D. C. Crick, B. V. V. Prasad, Y. Song, *J. Med. Chem.* **2011**, *54*, 4721–4734.
- [32] M. Andaloussi, L. M. Henriksson, A. Wieckowska, M. Lindh, C. Bjorkelid, A. M. Larsson, S. Suresh, H. Iyer, B. R. Srinivasa, T. Bergfors, T. Unge, S. L. Mowbray, M. Larhed, T. A. Jones, A. Karlen, *J. Med. Chem.* **2011**, *54*, 4964–4976.
- [33] A. M. Jansson, A. Wieckowska, C. Bjorkelid, S. Yahiaoui, S. Sooriyaarachchi, M. Lindh, T. Bergfors, S. Dharavath, M. Desroses, S. Suresh, M. Andaloussi, R. Nikhil, S. Sreevalli, B. R. Srinivasa, M. Larhed, T. A. Jones, A. Karlén, S. L. Mowbray, *J. Med. Chem.* **2013**, *56*, 6190–6199.
- [34] F. Gorrec, *J. Appl. Crystallogr.* **2009**, *42*, 1035–1042.
- [35] W. Kabsch, *Acta Crystallogr. Sect. D* **2010**, *66*, 125–132.
- [36] P. Evans, *Acta Crystallogr. Sect. D* **2006**, *62*, 72–82.
- [37] M. D. Winn, C. C. Ballard, K. D. Cowtan, E. J. Dodson, P. Emsley, P. R. Evans, R. M. Keegan, E. B. Krissinel, A. G. Leslie, A. McCoy, S. J. McNicholas, G. N. Murshudov, N. S. Pannu, E. A. Potterton, H. R. Powell, R. J. Read, A. Vagin, K. S. Wilson, *Acta Crystallogr. Sect. D* **2011**, *67*, 235–242.
- [38] G. N. Murshudov, A. A. Vagin, E. J. Dodson, *Acta Crystallogr. Sect. D* **1997**, *53*, 240–255.
- [39] T. A. Jones, J. Y. Zou, S. W. Cowan, M. Kjeldgaard, *Acta Crystallogr. Sect. A* **1991**, *47*, 110–119.
- [40] M. Harding, *Acta Crystallogr. Sect. D* **2006**, *62*, 678–682.
- [41] G. J. Kleywegt, T. A. Jones, *Methods in Enzymology*, Vol. 277, Academic Press, San Diego, **1997**, 525–545.
- [42] M. Harris, T. A. Jones, *Acta Crystallogr. Sect. D* **2001**, *57*, 1201–1203.
- [43] G. J. Kleywegt, M. R. Harris, J. Y. Zou, T. C. Taylor, A. Wahlby, T. A. Jones, *Acta Crystallogr. Sect. D* **2004**, *60*, 2240–2249.

Received: May 13, 2016

Revised: July 9, 2016

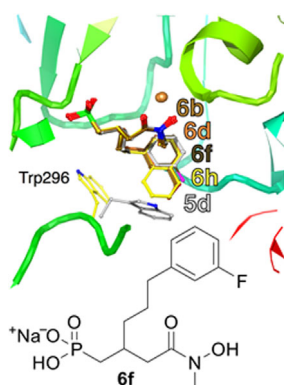
Published online on ■ ■ ■, 0000

FULL PAPERS

S. Sooriyaarachchi, R. Chofor,
M. D. P. Risseuw, T. Bergfors, J. Pouyez,
C. S. Dowd, L. Maes, J. Wouters,
T. A. Jones, S. Van Calenbergh,*
S. L. Mowbray*



**Targeting an Aromatic Hotspot in
Plasmodium falciparum 1-Deoxy-D-
xylulose-5-phosphate
Reductoisomerase with β -Arylpropyl
Analogues of Fosmidomycin**



Meta is better: X-ray structures show that arylpropyl substituents on β -phenylpropyl hydroxamate analogues of fosmidomycin displace a key tryptophan residue of the active site flap of Dxr, which then becomes largely disordered. For both *meta*- and *para*-substituted compounds, smaller substituents are associated with better potency; *meta*-substituted compounds such as **6 f** are usually better inhibitors, similar to the unsubstituted lead compound **5 d**.